



The characterization of plant derived-carbon dots and its responses on chlorophyll a fluorescence kinetics, radical accumulation in guard cells, cellular redox state and antioxidant system in chromium stressed-*Lactuca sativa*

Ceyda Ozfidan-Konakci^a, Evren Yildiztugay^{b,*}, Busra Arikan-Abdulveli^{b,**}, Fatma Nur Alp-Turgut^b, Canan Baslak^c, Murat Yildirim^b

^a Department of Molecular Biology and Genetics, Faculty of Science, Necmettin Erbakan University, 42090, Konya, Turkey

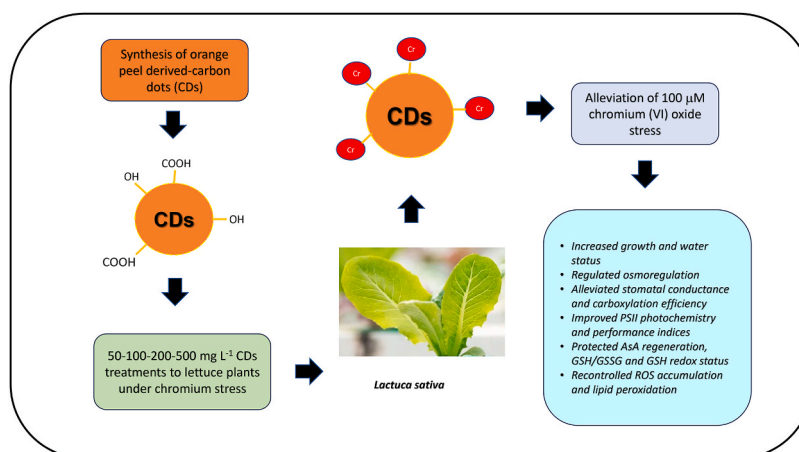
^b Department of Biotechnology, Faculty of Science, Selcuk University, 42130, Konya, Turkey

^c Department of Chemistry, Faculty of Science, Selcuk University, 42130, Konya, Turkey

HIGHLIGHTS

- CDs removed the Cr-reduced changes in RGR, RWC and Pro content.
- Cr toxicity decreased fluorescence kinetics and performance of PSII in lettuce.
- Cr disrupted the energy fluxes, quantum efficiency and performance index.
- All CD applications induced SOD and CAT in response to stress.
- CDs were able to protect the AsA regeneration, GSH/GSSG and GSH redox status.

GRAPHICAL ABSTRACT



ARTICLE INFO

Handling editor: Sagadevan Suresh

Keywords:
Antioxidant enzymes
Carbon dots

ABSTRACT

Based on their chemical structure and catalytic features, carbon dots (CDs) demonstrate great advantages for agricultural systems. The improvements in growth, photosynthesis, nutrient assimilation and resistance are provided by CDs treatments under control or adverse conditions. However, there is no data on how CDs can enhance the tolerance against chromium toxicity on gas exchange, photosynthetic machinery and ROS-based membrane functionality. The present study was conducted to evaluate the impacts of the different

* Corresponding author.

** Corresponding author.

E-mail addresses: cozfidan@erbakan.edu.tr (C. Ozfidan-Konakci), eytugay@selcuk.edu.tr (E. Yildiztugay), busra.arikan@selcuk.edu.tr (B. Arikan-Abdulveli), fatmanur.alp@selcuk.edu.tr (F.N. Alp-Turgut), cbaslak@selcuk.edu.tr (C. Baslak), muratyildirim@selcuk.edu.tr (M. Yildirim).

<https://doi.org/10.1016/j.chemosphere.2024.141937>

Received 18 August 2023; Received in revised form 8 March 2024; Accepted 5 April 2024

Available online 8 April 2024

0045-6535/© 2024 Elsevier Ltd. All rights reserved.

Chromium
Lactuca sativa
 Photosynthetic efficiency

concentrations of orange peel derived-carbon dots (50-100-200-500 mg L⁻¹ CD) on growth, chlorophyll fluorescence, phenomenological fluxes between photosystems, photosynthetic performance, ROS accumulation and antioxidant system under chromium stress (Cr, 100 μM chromium (VI) oxide) in *Lactuca sativa*. CDs removed the Cr-reduced changes in growth (RGR), water content (RWC) and proline (Pro) content. Compared to stress, CD exposures caused an alleviation in carbon assimilation rate, stomatal conductance, transpiration rate, carboxylation efficiency, chlorophyll fluorescence (F_v/F_m) and potential photochemical efficiency (F_v/F_o). Cr toxicity disrupted the energy fluxes (ABS/RC, TR_o/RC, ET_o/RC and DI_o/RC), quantum yields and efficiency (ΨE_o and ϕR_o), dissipation of energy (DI_o/RC) and performance index (PI_{ABS} and PI_{total}). An amelioration in these parameters was provided by CD addition to Cr-applied plants. Stressed plants had high activities of superoxide dismutase (SOD), peroxidase (POX) and ascorbate peroxidase (APX), which could not prevent the increase of H₂O₂ and lipid peroxidation (TBARS content). While all CDs induced SOD and catalase (CAT) in response to stress, POX and enzyme/non-enzymes related to ascorbate-gluthathione (AsA-GSH) cycle (APX, monodehydroascorbate reductase (MDHAR) and dehydroascorbate reductase (DHAR), the contents of AsA and, GSH) were activated by 50-100-200 mg L⁻¹ CD. CDs were able to protect the AsA regeneration, GSH/GSSG and GSH redox status. The decreases in H₂O₂ content might be attributed to the increased activity of glutathione peroxidase (GPX). Therefore, all CD applications minimized the Cr stress-based disturbances (TBARS content) by controlling ROS accumulation, antioxidant system and photosynthetic machinery. In conclusion, CDs have the potential to be used as a biocompatible inducer in removing the adverse effects of Cr stress in lettuce plants.

1. Introduction

Green synthesis of nanomaterials is gaining tremendous attention in nanotechnology. Green nanomaterials have been produced using biomolecules (proteins, enzymes and DNA), microorganisms (bacteria, fungi and algae) (Galal et al., 2021) or plant extracts (leaf, root, stem, fruit, flower and waste shell) (Amer et al., 2021). Biowaste plant materials are known as eco-friendly, non-corrosive, non-toxic, fully active upon recycling, and cost-efficient (Shahriari et al., 2019). In recent decades, much attention has focused on the synthesis and usage of carbon dots (CD) prepared from fruit peel wastes. The peels of corn stalk (Li et al., 2021b), banana (Atchudan et al., 2021), orange (Hu et al., 2021), watermelon and pomegranate (Muktha et al., 2020) are utilized. CDs have a small size (less than 10 nm), excellent photostability and, fluorescence performance, biodegradability, high biochemical reactivity, biocompatibility, low cytotoxicity, and water solubility (Guo et al., 2022a; Panahirad et al., 2023). CDs have advantages in gene transfection (Liu et al., 2012), drug delivery (Cheng et al., 2014), and bio-imaging (Fan et al., 2015). Recent finding reveals that CDs are easily uptake by the roots of plants and translocate to stems or leaves via the vascular system. The potential negative or positive impacts of CDs investigated varied depending on the CD concentrations (Li et al., 2020a). CD exposures significantly decreased biomass of roots and shoots, induced oxidative damage (lipid peroxidation) (1000–2000 mg L⁻¹ CD in maize), reduced the root elongation and down-regulated gene expression related to chloroplast function and structure (125–1000 mg L⁻¹ CD in *Arabidopsis*) (Chen et al., 2016, 2018). The plants subjected to CDs exhibit high capability of water and nutrient absorption of seeds, improved stem elongation and growth (optimal concentrations, 0.02–0.4 mg mL⁻¹), increased carbohydrate content, enhanced nitrogen fixation, and resistance against stress factors (Li et al., 2020a; Wang et al., 2018). There are different responses on chlorophyll content of CD applications, which increased in CD-applied mung beans (10, 50, 100, 500, 1000 μg mL⁻¹) (Zhang et al., 2018) and did not increase in rice under 0.56 mg mL⁻¹ CD (Li et al., 2018). To have more knowledge of agricultural systems, some points still need to be clarified in practical applications. CDs can improve the photosystem capacity by enhancing the electron transfer rate. Owing to their excellent optical properties, CDs are considered an alternative candidate as energy acceptors and donors in inorganic or organic hybrid structures (Hildebrandt et al., 2017). The process of light harvesting, which is sensitive to extreme conditions, is a basic issue for photosynthesis in plants (Kundu and Patra, 2017) and researchers have tried to find a way for accelerating light harvesting capacity by synthetic methods. LeBlanc et al. (2014) described a hybrid system in which graphene-based CDs interact with the reaction center of the photosystem I (PSI). Thanks to this hybrid

system, it has been shown that light harvesting can be done in a wider wavelength range of photosynthesis. In the other study, Nabiev et al. (2010) represented that the excitation energy harvested by CDs was transferred to reaction centers of PSII. The nitrogen-enriched dots, which are applied as fertilizer, can enhance the fluorescence ability of photosynthetic pigments by energy transfer from CDs (Budak et al., 2020). Based on a study in lettuce and tomato presented by Kou et al. (2021), CD applications resulted in a promotion on photosynthesis by activated PSI, thus improving nutrient status of plants. The mechanisms underlying CDs in terms of photochemical reactions and photosystems efficiency need further clarification.

Another attractive property of CDs is the capacity for both production and elimination of reactive oxygen species (ROS). The reason for the scavenging capacity of CDs under stress conditions is the electron donor and acceptor amino and carboxyl groups on the surface (Zhao et al., 2015). After drought exposure, CDs triggered the resistance of peanuts by activating antioxidant enzymes such as peroxidase (POX), superoxide dismutase (SOD), and catalase (CAT) and decreased lipid peroxidation (malondialdehyde content) (Su et al., 2018). Enhancing the antioxidant system reflects tolerance in response to adverse conditions (Kou et al., 2021). In the presence of heavy metal toxicity such as cadmium, the inhibition of cadmium absorption into the plants, promotion of anthocyanin content and antioxidant system, and alleviation of membrane damage were observed in CD-applied wheat and citrus seedlings (Li et al., 2019). CD supplementation caused low arsenic accumulation via the decline of arsenic uptake in *Cicer arietinum* roots (Chandrakar et al., 2020a). Xiao et al. (2019) reported a reduction in cadmium accumulation upon 50 and 75 mg L⁻¹ CD in wheat roots and an increase in chlorophyll content under 50 mg L⁻¹ CD. Since the positive effects of CDs on the metabolic process in plants subjected to heavy metal toxicity, we have been considered as an alternative tool for the CD-mediated removal of chromium-toxicity in lettuce plants. Chromium-mediated pollution caused a decrement in photosynthesis, cell respiration, pigment biosynthesis, transpiration rate, nutrient uptake and cell division in plants (Ma et al., 2016; Zhao et al., 2019). Chromium (Cr) exposures are found to induce oxidative stress, which is eliminated through antioxidant system and accumulation of osmolytes or some protecting peptides such as phytochelatin (Christou et al., 2020). However, there is still some question concerning the interactions of CDs in plants under Cr stress, particularly how CDs, can be used as a fertilizer, regulate the antioxidant system and photosynthetic apparatus to reduce damage induced by Cr stress. Therefore, the innovative point of this study is the detailed assessments on the defense response systems and kinetics of chlorophyll fluorescence and photochemical activity in photosystems of plants after CDs and Cr stress exposure.

Lactuca sativa, the most consumed leafy vegetable, has been selected

as an ecotoxicological crop model due to its high metal-accumulating ability such as cadmium (Li et al., 2020b). However, there is no knowledge about the defense mechanisms of CDs against Cr stress in lettuce plants. To close the gap in information regarding the possible positive impacts of CDs, the roles of different concentrations of orange peel derived-carbon dots (50-100-200-500 mg L⁻¹ CD) were clarified by integrating the growth, water relations (water content and proline content), gas exchange (stomatal conductance, transpiration rate, carboxylation efficiency and intercellular CO₂ concentrations), chlorophyll fluorescence, the photochemical capacity of PSII, ROS accumulation (H₂O₂ content), antioxidant system (enzyme activities and ascorbate-glutathione cycle) and lipid peroxidation in chromium (100 µM Cr)-treated *Lactuca sativa*. The novelty of the current study is revealing the antioxidant capacity, photochemical efficiency, gas exchange and redox state of plant-based CD applications in controlling Cr-induced oxidative damages in *Lactuca sativa*.

2. Material and methods

2.1. Materials and synthesis of orange peel derived-carbon dots

All chemicals used in this study were commercially purchased and used as pure grade without further purification. Orange was purchased from the market. Ethylene diamine (99%, EDA) and filter papers were purchased from Sigma-Aldrich. Milli-Q water was used in all synthesis and to prepare solutions for characterization studies.

2.2. Synthesis of orange peel derived-carbon dots

Purchased fresh oranges were sterilized 3 times with distilled water after pre-washing. The orange peels were peeled and cut into fine pieces and ground with a laboratory grinder. The ground shells were left to dry in an oven at 70 °C for 1 h. 3 g of dried shells were weighed and a solution of 60 ml of distilled water was prepared. The prepared solution was stirred for 1 h in a magnetic stirrer at 400 rpm and 40 °C until it became homogeneous. A separatory funnel was used to separate the oil phase in the orange peel solution. The orange peel sample separated from its oily layer was ultracentrifuged 3 times at 10,000 rpm for 15 min. The sample obtained after ultracentrifugation was taken into 60 ml microwave Teflon and 2 ml of Ethylenediamine (EDA) was added to the Teflon. Microwave treatment was applied at 90 °C for 20 min. In order to purify the sample obtained after microwave synthesis, stepwise ultracentrifugation and syringe filtering processes were applied. After 15 min of ultracentrifugation at 10,000 rpm, the sample was passed through the syringe filter. This process was repeated 3 times. The transparent sample was dried in a magnetic stirrer at 60 °C.

2.3. The characterization of orange peel derived-carbon dots

Fluorescence spectroscopy measurements of the CDs and lettuce plant were made by using PerkinElmer LS 55 brand Luminescence Spectrometer. FT-IR and XRD were used to perform structural characterizations of CDs and the plant samples with CDs. Fourier transformed infrared (FT-IR) spectra were recorded from 400 to 4000 cm⁻¹ by using Bruker Fourier Transform Infrared FT-IR (ATR) Bruker Advance D8 brand. X-ray Diffraction Spectroscopy (XRD) was used to determine the crystallinity of CDs and CDs in lettuce plant. Dynamic light scattering (DLS) analysis was performed with a MALVERN/DLS MPT2 instrument to measure the intensity and variation of light scattered from small particles in dilute solution of CDs. A JEOL JEM-2100PLUS TEM brand transmission electron microscopy (TEM) studies were performed to justify the formation of the CDs. After weighing 1 g of powdered plant samples, 1.5 ml of water was added to them. The solutions were left to stir for one day. The next day, the solutions were filtered to separate them from the residue fractions. 500 µl of the filtered solutions were pipetted and placed in a mixing bowl. Pure water was added to the

solutions until the total volume was 2 ml and measurements were made by fluorescence spectroscopy. CD stock solution was prepared at a concentration of 5 mg ml⁻¹. The prepared stock solution was first diluted in half with water. The prepared solution was re-diluted with water at a 1:2 (CD solution:water) volume ratio and this solution was used for fluorescence measurement. FT-IR and XRD measurements were made directly using powdered CD and plant samples.

2.4. Plant material and the applications of Cr stress/CDs and the sampling

Lettuce seeds (*Lactuca sativa* L. cv. *paris island*) were surface sterilized and allowed to germinate on wet filter paper. After one week, seedlings were transferred to Hoagland solution under controlled conditions and it was refreshed every other day. All treatments were completed by being dissolved in Hoagland solution and were added to the growth medium for seven days. For stress treatment, the lettuce plants were exposed to chromium dichloride (Cr, 100 µM chromium (VI) oxide). After the synthesis stage of CDs, orange peel derived-carbon dots (50-100-200-500 mg L⁻¹ CD) were subjected to lettuce plants as simultaneously with Cr stress. The treatment doses were selected according to previous findings (Ahmad et al., 2020; Prakash et al., 2022; Tan et al., 2021; Wang et al., 2021). Lettuce plants were harvested after one week of treatment.

2.5. Elemental analysis

The endogenous contents of Cr⁶⁺, Ca²⁺, K⁺, Mg²⁺, Fe²⁺ and Mn²⁺ were analyzed by ICP-AES (Varian-Vista) and the measurements were completed for third leaf (0.1 g dry weight) (Nyomora et al., 1997).

2.6. Determination of growth and water relations

Hunt et al. (2002) proposed a method for determining relative growth rate (RGR). Following treatment, six leaves from each group were harvested and their relative water content (RWC) was calculated using the Maghsoudi et al. (2019) algorithm. Proline (Pro) content was determined in 0.5 g fresh samples followed by Chandrakar et al. (2016).

2.7. Determination of gas exchange parameters

Carbon assimilation rate (A), stomatal conductance (g_s), intercellular CO₂ concentration (C_i) and transpiration rate (E) were detected with a portable gas exchange system (LCpro⁺; ADC, Hoddesdon, UK). The stomatal limitation value (L_s) was calculated as 1 - C_i/C_a (Ma et al., 2011).

2.8. Determination of photosynthetic efficiency and OJIP analysis

A portable fluorometer (Handy PEA, Hansatech Instruments Ltd., Norfolk, UK) was used to determine the maximal quantum yield of PSII photochemistry (F_v/F_m), physiological state of the photosynthetic apparatus (F_o/F_m) and potential photochemical efficiency (F_v/F_o). Handy PEA (Plant Efficiency Analyzer, Hansatech Instruments Ltd.) was used to reveal the alterations in the photochemistry of PSII. The descriptions for the estimated parameters are included in Supplementary Table S1.

2.9. Determination of oxidative stress biomarker assays and confocal laser scanning microscopy

H₂O₂ content in leaves was evaluated using the method described by Velikova et al. (2000), and lipid peroxidation level (TBARS content) was computed using the method described by Rao and Sresty (2000). H₂O₂ concentration in guard cells was observed using 2,7-dichlorofluorescein diacetate (H₂DCF-DA), as explained previously (Ahmed et al., 2020).

2.10. Determination of antioxidant system and AsA-GSH cycle enzyme/non-enzyme compositions

For protein and enzyme extractions, 0.5 g of each leaf sample was homogenized in 50 mM Tris-HCl (pH 7.8) containing 0.1 mM ethylenediaminetetraacetic acid (EDTA), 0.2% Triton X-100, 1 mM phenylmethylsulfonyl fluoride and 2 mM dithiothreitol (DTT) (Li et al., 2020a, b). The total soluble protein content of the enzyme extracts was determined (Bradford, 1976). Superoxide dismutase (SOD) isozyme/enzyme

activity was defined (Beauchamp and Fridovich, 1971; Laemmli, 1970). The activity of catalase (CAT) isozyme/enzyme was determined using the procedure suggested by Woodbury et al. (1971) and Bergmeyer (1970). The isozymes/enzyme capacity of peroxidase (POX) was measured according to the method suggested by Seevers et al. (1971) and Herzog and Fahimi (1973). The enzyme/isozyme activities of glutathione S-transferase (GST) and glutathione peroxidase (GPX) were determined (Hossain et al., 2006; Ricci et al., 1984). The isoforms and total NADPH oxidase (NOX) activity were calculated (Jiang and Zhang,

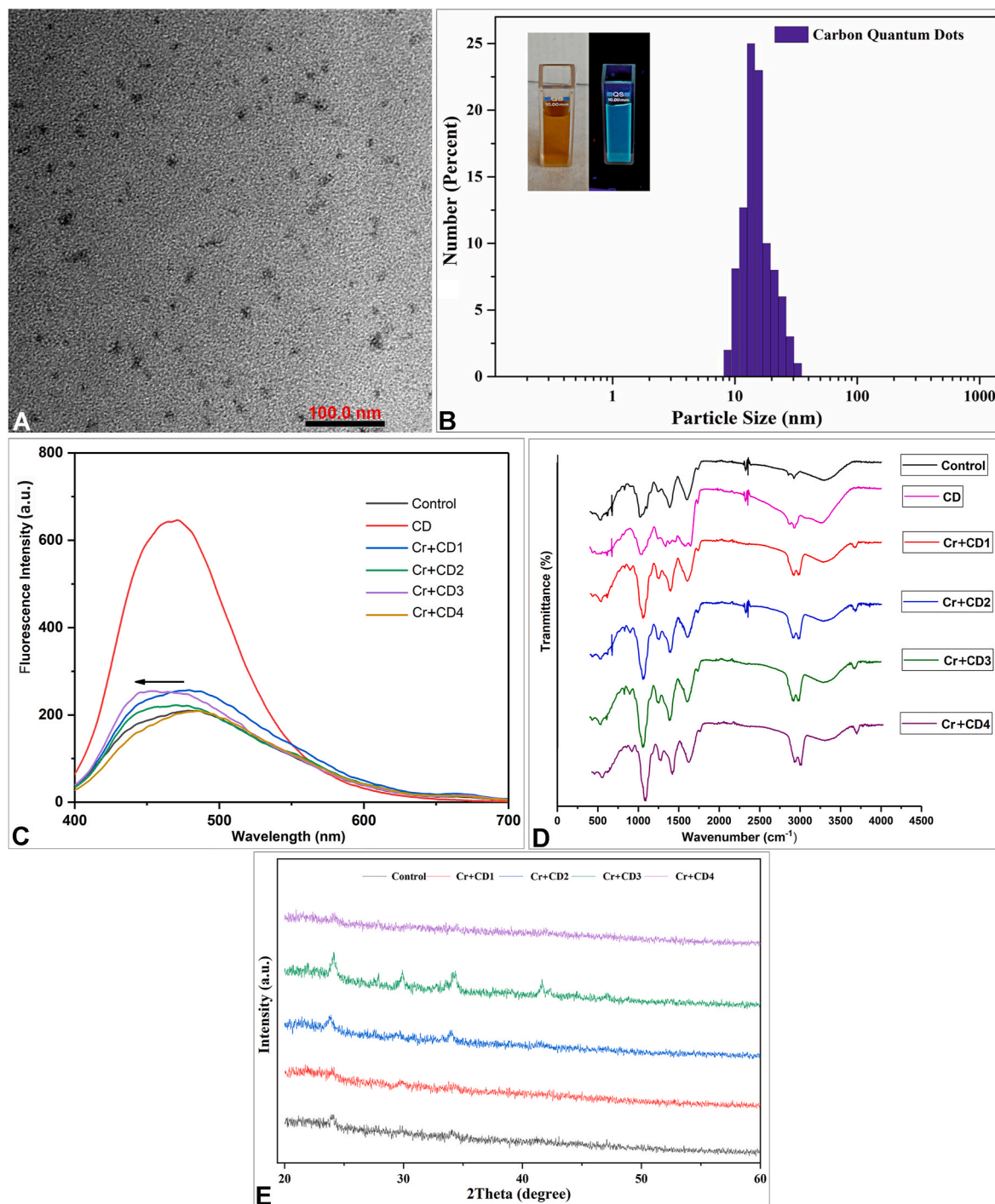


Fig. 1. The characterization of orange peel derived-carbon dots (50-100-200-500 mg L⁻¹ CD) in lettuce plants under chromium (VI) oxide (100 μM Cr). **(A)** TEM image of CDs, **(B)** DLS measurements of CDs, **(C)** Fluorescence spectra of control group, CD, Cr + CD1, Cr + CD2, Cr + CD3 and Cr + CD4, **(D)** FT-IR spectra of control group, CD, Cr + CD1, Cr + CD2, Cr + CD3 and Cr + CD4, **(E)** XRD graphics of CD, Cr + CD1, Cr + CD2, Cr + CD3 and Cr + CD4. (For interpretation of the references to colour in this figure legend, the reader is referred to the Web version of this article.)

2002; Sagi and Fluhr, 2001).

Ascorbate peroxidase (APX) and glutathione reductase (GR) were spectrophotometrically and electrophoretically carried out (Mittler and Zilinskas, 1993; Nakano and Asada, 1981). The contents of ascorbate (AsA) and oxidized ascorbate (DHA) were estimated (Dutilleul et al., 2003). The procedure for monodehydroascorbate reductase (MDHAR) and dehydroascorbate reductase (DHAR) was performed (Dutilleul et al., 2003). Glutathione (GSH) was assayed according to Paradiso et al. (2008), utilizing aliquots of supernatant neutralized with 0.5 M K-P buffer. Based on enzymatic recycling, glutathione is oxidized by DTNB and reduced by NADPH in the presence of GR, and glutathione content is evaluated by the rate of absorption changes at 412 nm. Oxidized glutathione (GSSG) was determined after the removal of GSH by 2-vinylpyridine derivatization. Standard curves with known concentrations of GSH and GSSG were used for the quantification. GSH redox status was obtained (Shi et al., 2013).

The Gel Doc XR + System was used to photograph stained gels and subsequently evaluated using Image Lab software v4.0.1 (Bio-Rad, California, USA). Enzyme standards are used in gels for normalization.

2.11. Statistical analysis

All data were reported as technical triplicates and six biological replicates. One-way analysis of variance (ANOVA) was used for all analyses. SPSS 20.0 was used to perform statistical analysis on the values. At $p < 0.05$, differences were considered significant. In all figures, the error bars represent standard errors of the means.

3. Results

3.1. Orange peel derived-CDs under Cr stress: Characterization

TEM image showing information about the particle size and morphology of CDs can be seen in Fig. 1A. Although the particle size of CDs varies between 10 nm and 24 nm, the majority of the population has a size of 17 nm. The shape of the particles is typically flattened from the sides and not fully spherical. Fig. 1B shows the size analysis of CDs with DLS (Le et al., 2023; Liu et al., 2017; Oliveira et al., 2020; Siddique et al., 2018). According to the DLS results, the size and standard deviation of the obtained particles were found to be 17.423 ± 7.592 nm. This study reported the single-pot synthesis of CDs from orange peels. When the results are examined, the fluorescence peak width, FTIR peaks and the range of the peak in the spectrum obtained for XRD are exactly compatible with the results obtained from orange in the literature (Liang et al., 2017; Prasannan and Imae, 2013).

Fig. 1C showed the fluorescence spectra of the control group, CDs in pure form, Cr + CD1, Cr + CD2, Cr + CD3, Cr + CD4. In order to obtain samples as control group, Cr + CD1, Cr + CD2, Cr + CD3, and Cr + CD4, the powders taken from different parts of lettuce were mixed and were dissolved in water. Fluorescence spectroscopy was used to measure the liquids obtained after the sediment was filtered. A solution of appropriate concentration was prepared from the powder form of pure CDs that were not given to the plants, and fluorescence measurements were compared with the emissions of samples taken from lettuce plants. According to Fig. 1C, the obtained carbon dots show a strong emission spectrum at around 475 nm. The resulting peak has a very symmetrical and sharp peak. On the other hand, it is seen that the control group has a rather broad emission and low intensity emission peak. Considering the fluorescence peaks obtained for the samples with Cr and CD together from lettuce plants, it is seen that the top of the peaks is suppressed and shifted to the left. The peak starts to appear around 450 nm. The binding relationship between Cr and CD is thought to cause this result. Especially for 200 mg L^{-1} CD (CD3) of carbon quantum dot concentration, the peak on the left is more prominent than the other spectra. It has been determined that this value is the concentration that minimizes the stress on the plant by the application of different CD concentrations. As in our

current study, there are examples of studies on the interactions of Cr and CDs in the literature. In the example of an optical sensor study developed for Cr (VI) ions, the interaction between Cr and CDs was confirmed according to the results obtained by fluorescence spectroscopy. The composition of CDs and concentration of Cr (VI) ions can also affect the change of these optical properties of CDs. In conclusion, CDs obtained from an orange waste enabled the binding of Cr (VI) ions because they contained both amine and carboxyl groups. For this reason, a change was observed in the fluorescence intensity graphs according to the Cr ion concentration. It has been reported that there were energy changes in the absorption peaks of carbon dots due to the binding of Cr ions to the surface of carbon dots (Liang et al., 2017; Moonsuang et al., 2020; Zhang et al., 2017).

As depicted in Fig. 1D, the FT-IR spectrum displayed the appearance of different peaks that represent some functional groups located on the surface of CDs. In order to investigate the mechanisms of CDs against Cr stress in lettuce plants, samples taken from lettuce plants were measured by FT-IR spectroscopy. As can be understood from the spectra, the peaks seen in the control group are also seen in the spectra obtained for Cr + CD1, Cr + CD2, Cr + CD3 and Cr + CD4 samples. Although there is a small shift in the location of the peaks, around 1010 cm^{-1} peaks in the control group shifted to around 1030 cm^{-1} in the sample taken from the CD-treated plant and this peak belongs to the C-C bonds. The control group spectrum exhibited a band at 1238 cm^{-1} that could be related to stretching vibrations of C-N. This peak is seen to be intensified in the plant with N-CD (Cr + CD1, Cr + CD2, Cr + CD3 and Cr + CD4). The spectrum exhibited bands of CDs at 3280 and 2925 cm^{-1} that could be related to stretching vibrations of N-H and C-H. Compared to the vibration peaks attributed to C-H in the control group, the intensity of these peaks increased in plant samples given CDs and Cr (Chandrasekaran et al., 2020). Also, the peak of CDs at 1635 cm^{-1} is due to the stretching vibration of C=C and C=O. The peaks at 1389 cm^{-1} and 1575 cm^{-1} in the spectrum of CDs are thought to be caused by asymmetric and symmetric stretching vibrations of carboxylate anions. These peaks are also seen in the FT-IR spectra of the samples in which CDs were given to the plant. Absorption peaks of $500\text{--}945 \text{ cm}^{-1}$ are associated with the bending vibration of C-H in the structure of the control group, CDs, and lettuce plant with CD (Su et al., 2017).

X-ray Diffraction Spectrometer (XRD) analysis for qualitative and quantitative examinations of CDs was performed with BRUKER D8 ADVANCE X-Ray Diffractometry. The XRD model of CDs was shown in Fig. 1E. Peaks corresponding to the (0 0 2) plane were shown at $2\theta = 23.20^\circ$ and 24.80° for the CD, $2\theta = 24.10^\circ$ for the Control, $2\theta = 20.60^\circ$, 22.01° and 24.02° for the Cr + CD1, $2\theta = 23.85^\circ$ for the Cr + CD2, $2\theta = 24.14^\circ$ for the Cr + CD3, $2\theta = 20.08^\circ$ and 24.18° for the Cr + CD4. According to literature, the broad peaks at $2\theta = 20.60^\circ$ (Bajpai et al., 2019; Lu et al., 2016), $2\theta = 22.01^\circ$ (Sabet and Mahdavi, 2019), $2\theta = 23.20^\circ$ and 23.85° (Qu et al., 2012), and $2\theta = 24.10^\circ$ and 24.18° (Jaison et al., 2023) indicate the existence of CDs.

3.2. Orange peel derived-CDs under Cr stress: The accumulation of some ions

As expected, Cr treatment induced the endogenous content of Cr^{6+} in lettuce plants by a 1.1-fold increase (Fig. 2A). This induction in Cr^{6+} content by stress was reduced by all CD applications. Cr stress caused less accumulation in the endogenous contents of Ca^{2+} (Fig. 2B), K^+ (Fig. 2C), Mg^{2+} (Fig. 2D) and Mn^{2+} (Fig. 2F) in lettuce leaves. However, no alteration in the endogenous content of Fe was observed under stress conditions (Fig. 2E). The limitations on these ion contents were removed by all CD applications, except for Ca^{2+} content at Cr + CD1. The promoted accumulation in the contents of Ca^{2+} , Mg^{2+} , Fe^{2+} and Mn^{2+} was detected after CDs alone as compared to the control group.

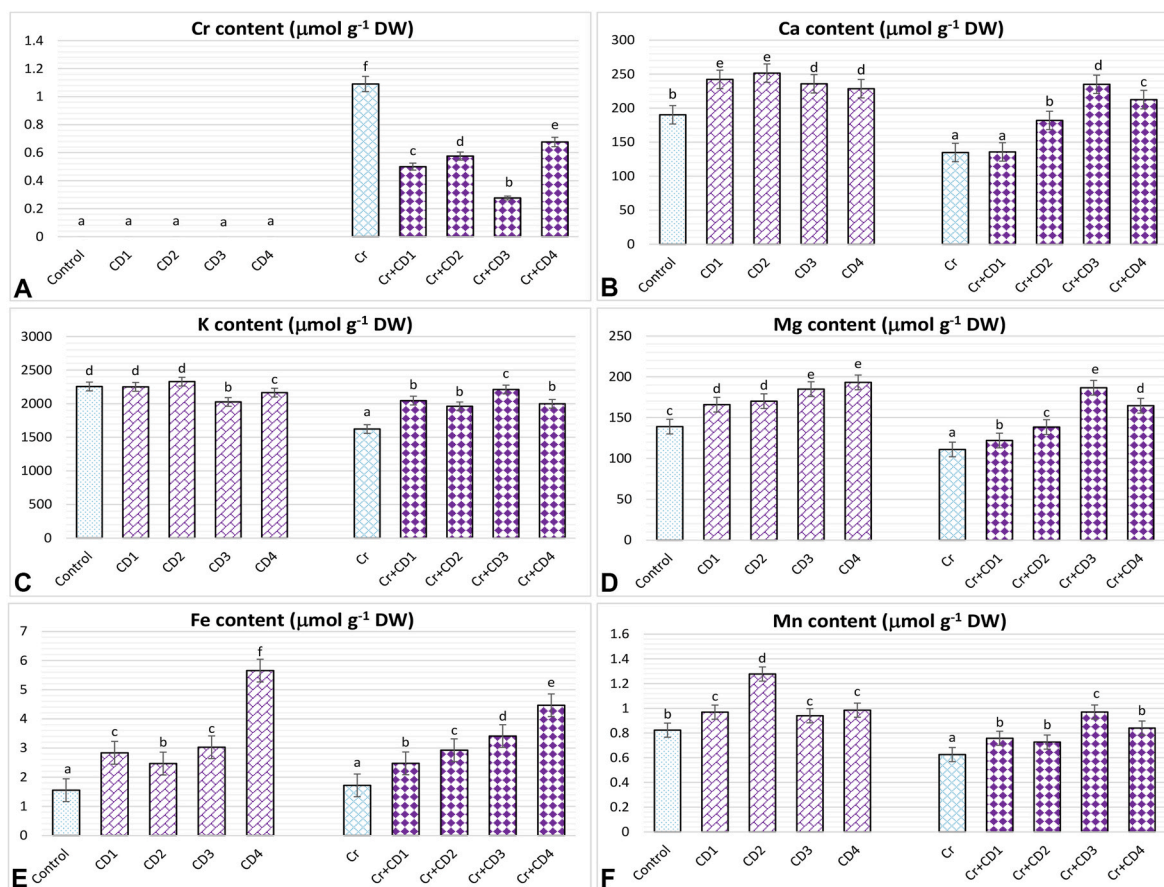


Fig. 2. The effects of orange peel derived-carbon dots (50-100-200-500 mg L^{-1} CD) on the endogenous content of (A) Cr^{6+} , (B) Ca^{2+} , (C) K^+ , (D) Mg^{2+} , (E) Fe^{2+} and (F) Mn^{2+} in lettuce plants under chromium (VI) oxide ($100 \mu\text{M Cr}$). (For interpretation of the references to colour in this figure legend, the reader is referred to the Web version of this article.)

3.3. Orange peel derived-CDs under Cr stress: Growth and water relations

Fig. 3A showed that there was a significant decline in RGR under Cr stress (by a 1.6-fold reduction). The presence of CDs provided high levels of RGR after Cr stress or non-stress conditions. Stress led to a considerable decrease (by a 27% decline) in the RWC of lettuce plants (Fig. 3B). Like RGR, the decreased values of RWC were reversed by plant-based CD applications in response to the control or stress conditions. Cr stress did not affect Pro content compared to the control group (Fig. 3C). The co-existence of CDs and Cr stress resulted in an increase in Pro content (Fig. 3C). This trend in Pro occurred only when plants were exposed to 50 mg L^{-1} CD under the control conditions.

3.4. Orange peel derived-CDs under Cr stress: Gas exchange parameters

Cr-applied lettuce plants had a considerable decline in the carbon assimilation rate (A), which was a maximum reduction by 4-fold (Fig. 4A). Both CD alone and CD together with Cr stress increased A levels compared to that of the control and stress alone group, respectively. Stomatal conductance (g_s) was noticeably decreased under $100 \mu\text{M Cr}$ toxicity (Fig. 4B). Except for Cr + CD1, the high levels in g_s were calculated under the combination of CD and Cr stress. g_s values did not reach to the control groups at CD alone. Cr exposure suppressed the intercellular CO_2 concentration (C_i) to its lowest levels by a 40% decrease (Fig. 4C). Compared to the stress alone, more reduction in C_i was observed through exogenously applied CDs. A similar response in C_i was detected at CD alone as compared to the control group. The reduction of transpiration rate (E) was observed under stress exposure (Fig. 4D). Besides, this decline in E was prevented by CD applications

under Cr stress, except for Cr + CD1. Co-exposure to CDs and Cr toxicity resulted in significant decreases in E levels. The stomatal limitation value (L_s) increased in lettuce plants with Cr stress (Fig. 4E). However, this limitation in stomatal regulation was removed by all CD concentrations in *L. sativa*. By comparison, there was no difference in L_s between CD alone and the control group. While the low levels of carboxylation efficiency (A/C_i) were detected in Cr-treated plants, the co-existence of CDs and Cr caused a higher ratio in A/C_i .

3.5. Orange peel derived-CDs under Cr stress: Chlorophyll fluorescence

Fig. 5 revealed that Cr exposure significantly inhibited F_v/F_m and F_v/F_o of lettuce leaves and the highest reduction level in F_v/F_o was by a 37% decline. However, stress resulted in a noticeable induction in F_o/F_m . When lettuce plants were applied to CDs together with Cr stress, remarkable changes were created on F_v/F_m (Fig. 5A), F_o/F_m (Fig. 5B) and F_v/F_o (Fig. 5C). The findings for these parameters were reversed by all CD treatments. On the other hand, no impact on F_v/F_m , F_o/F_m and F_v/F_o was detected after CD applications under the control conditions (except for 500 mg L^{-1} CD in F_v/F_o).

3.6. Orange peel derived-CDs under Cr stress: Chlorophyll-a fluorescence transient

The phenomenological energy fluxes of the treatment groups were presented in Fig. 6A. In response to Cr stress, the promoted levels of ABS/RC , TR_o/RC and DI_o/RC related to absorption, energy trapping and dissipation of reaction centers and the low level of ET_o/RC showing electron transport of reaction centers were detected under stress

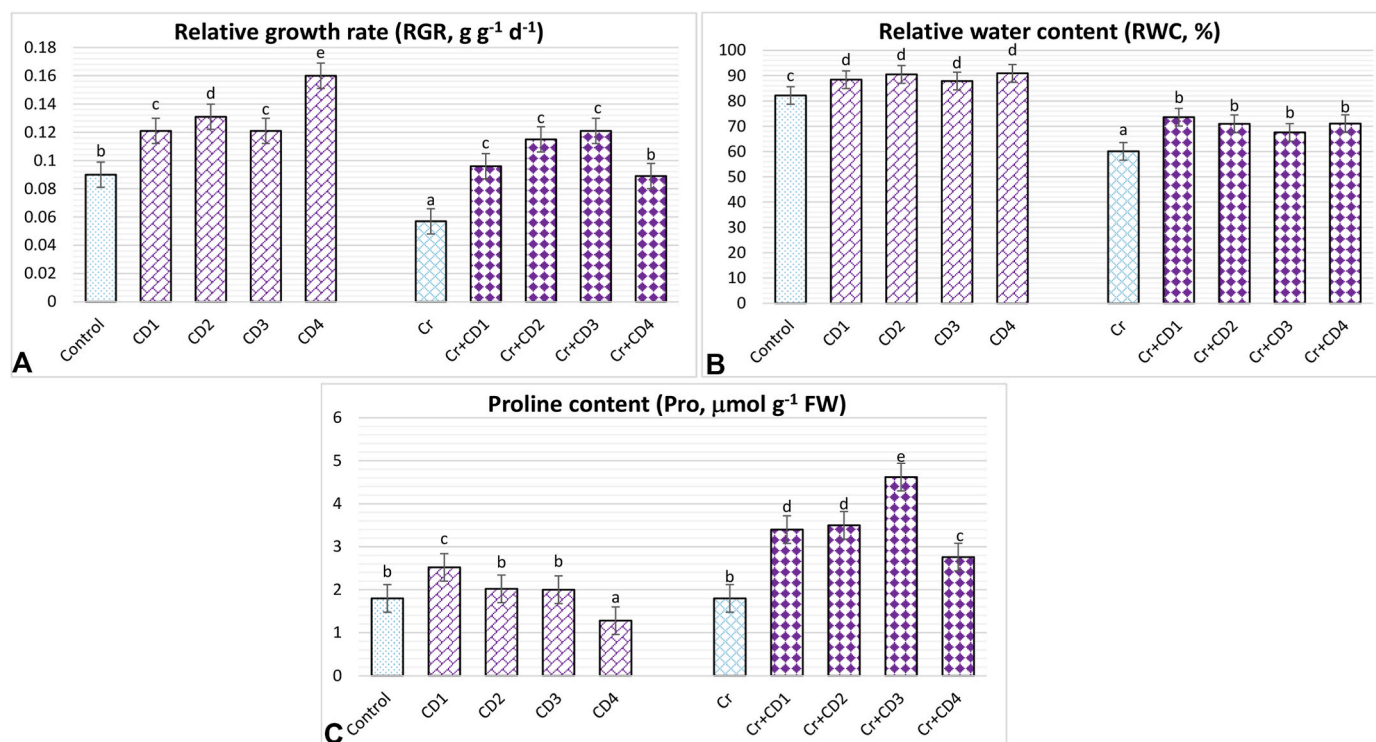


Fig. 3. The effects of orange peel derived-carbon dots (50-100-200-500 mg L⁻¹ CD) on (A) relative growth rate (RGR), (B) relative water content (RWC), (C) proline content (Pro) in lettuce plants under chromium (VI) oxide (100 μM Cr). (For interpretation of the references to colour in this figure legend, the reader is referred to the Web version of this article.)

treatment. The stress-dependent negative effects on reaction centers were reversed by all CD concentrations. The induced dV/dt_0 under stress showed the closure rate of reaction centers. On the other hand, Cr stress decreased $\Phi P_0/(1-\Phi P_0)$, $\Psi E_0/(1-\Psi E_0)$ and $\gamma RC/(1-\gamma RC)$ indicating the efficiency of light reaction and rate of biochemical reaction in lettuce plants. All negative changes in the photosynthetic apparatus were removed by CD applications. Quantum efficiency-related parameters (ΨE_0 and ΦR_0) reduced by Cr stress were increased by CD applications. The induced relative variable fluorescence (V_I and V_J) representing the electron transfer at the acceptor side of PSII increased in Cr-applied lettuce plants. However, CDs supplied a reduction in these parameters compared to the stress alone. The performance indices (PI_{total} and PI_{ABS}) for energy conservation from photons absorbed by PSII to the reduction of PSI end acceptors calculated a markedly reduction after stress exposure, which was not observed under the combination of CDs and Cr toxicity. CD alone provided high levels of the photosynthetic index. The heat map given in Fig. 6B summarized the plant responses to Cr and/or plant-derived CD applications.

3.7. Orange peel derived-CDs under Cr stress: ROS accumulation and lipid peroxidation

The accumulation of H₂O₂ was measured by a 2, 7-dichlorofluorescein diacetate (H₂DCF-DA) staining (Fig. 7A) and spectrophotometry-based method (Fig. 7B). DCF-DA staining showed that the fluorescence signal (green spots) increased in stoma of Cr-applied lettuce plants (Fig. 7A). As evident by the data in Fig. 7A, the high content of H₂O₂ (by 1.9-fold increase) was calculated in plants treated with stress (Fig. 7B). As compared to the stress alone, CD addition to stressed plants resulted in the low H₂O₂ levels. This result was consistent with the reduced intensity of H₂O₂ fluorescence under Cr stress plus CDs. As compared to the control group, CD exposures had no effect on the contents of H₂O₂ (Fig. 7B) and TBARS (Fig. 7C). Similar to H₂O₂ content, a 5-fold increase in TBARS was determined under Cr stress. This trend in TBARS was

prevented by all CD applications (Fig. 7C).

3.8. Orange peel derived-CDs under Cr stress: Antioxidant defense system and AsA-GSH cycle

As revealed in Fig. 8A, three SOD isozymes (one Mn-SOD and two Fe-SOD1-2) were detected in lettuce leaves during the experimental period. In all treatment groups, Cu/Zn-SOD could not be detected. Total SOD activity of leaves increased in the presence of Cr stress (Fig. 8A), which was compatible with the intensities of Fe-SOD1-2 (Fig. 8B). This induction in SOD was maintained by plant-derived dots in lettuce plants. However, no change in this activity showed under CD alone. As illustrated by Fig. 8C, only one CAT isozyme was viewed by native PAGE analysis. While total CAT activity was similar to the control groups (Fig. 8D), CD applications caused higher activity than that of Cr stress. On the other hand, under CD4 alone, the increment in both total and isozyme activities of CAT was clearly observed in lettuce leaves.

The plants exhibited three POX isoforms under all treatment groups (Fig. 9A). As compared to the control group, POX activity induced Cr-applied plants by a 2-fold increase (Fig. 9B), depending on all POX isozymes (Fig. 9A). Except for Cr + CD4, the increments in the intensities of POX2-3 were consistent with the total POX activity in CDs plus Cr-treated plants. There was an increase in POX activity by CD applications under non-stress conditions. Examination of APX isoenzymes identified three isoforms (APX1-2-3) (Fig. 9C). The high activity in APX was observed under stress treatment (Fig. 9D). CD1-2-3 applications to stress-applied plants supplied the further increase in total APX activity, which were related to the changes in all APX intensities. After CD exposure to lettuce plants, APX activity increased throughout the experimental period.

Quantification of the band intensities showed two isoforms of GR (GR1-2) in lettuce leaves (Fig. 10A). Both CDs alone and Cr stress decreased total GR activity compared to the control group (Fig. 10B). When the combination of CD and Cr stress applied, the intensities of GR1

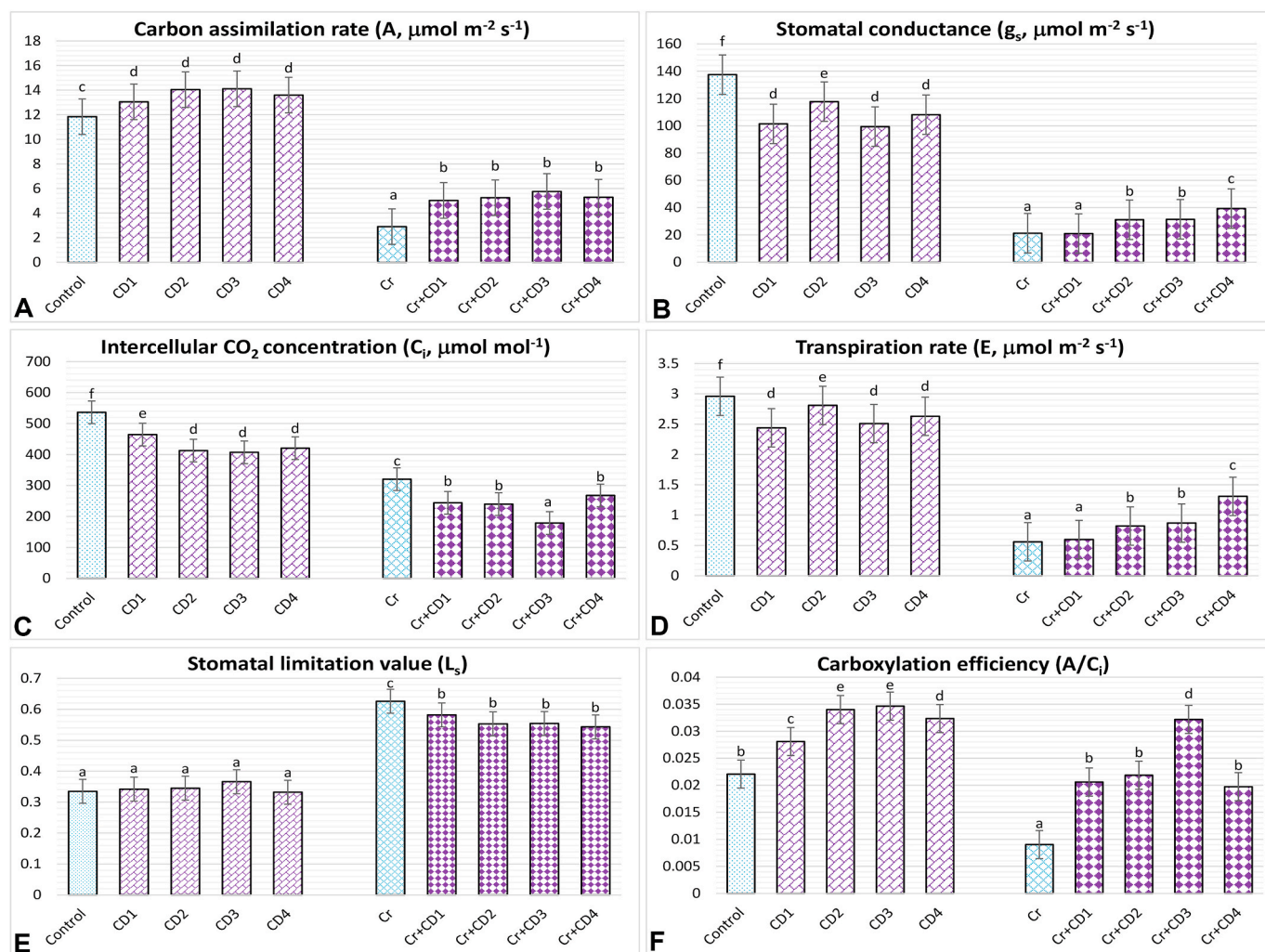


Fig. 4. The effects of orange peel derived-carbon dots (50-100-200-500 mg L^{-1} CD) on (A) carbon assimilation rate (A), (B) stomatal conductance (g_s), (C) intercellular CO_2 concentration (C_i), (D) transpiration rate (E), (E) stomatal limitation value (L_s), (F) carboxylation efficiency (A/C_i) in lettuce plants under chromium (VI) oxide (100 μM Cr). (For interpretation of the references to colour in this figure legend, the reader is referred to the Web version of this article.)

and GR2 were stronger than stress treatment alone, except for Cr + CD1. As shown in Fig. 10C, four NOX isoenzymes (NOX1-2-3-4) were detected by native PAGE analysis. The total NOX activity decreased by a 2.5-fold decline under the stress treatment (Fig. 10D). This reduction of NOX activity was especially related to the intensities of NOX1-3-4. Cr + CD1-2-3 was either lower or unaffected the total NOX activity as compared to the Cr stress alone. Similar to the GR activity, a remarkable decrease was measured in NOX of lettuce leaves.

During the experimental period, six isoforms for GST enzyme (GST1-2-3-4-5-6) were defined by gel analysis (Fig. 11A). The total GST activity was higher in Cr stress-treated plants, providing the intensities of GST2-3-4-6. Under stress or non-stress conditions, exogenous CD application could maintain the high levels of total GST activity (Fig. 11B). This effect was associated with the induced intensities of GST2-3-4. The isozyme staining pattern in Fig. 11C showed that the lettuce leaves treated with stress and/or CDs had three GPX isozymes (GPX1-2-3). Unaffected activity in GPX was observed under Cr stress (Fig. 11D). However, after Cr exposure, plant-derived CDs provided a significant increase in GPX enzyme activity, which was responsible for the intensities of GPX2-3. A similar response was calculated in the CD alone-applied plants. CD2 caused the maximum induction in GPX activity under stress or non-stress treatments.

There was a similar trend between MDHAR and DHAR activities throughout the experimental period (Fig. 12A–B). Both MDHAR and

DHAR decreased in the presence of stress by 2- and 1.2-fold decrement, respectively. Cr stress together with CDs caused an induction in MDHAR and DHAR, except for Cr + CD4 as compared to the stress alone. Under the existence of non-stress, CD1-2-3 alone maintained the high activities of MDHAR and DHAR. Interestingly, CD4 alone and Cr + CD4 created no increase in these enzyme activities. While there was no effect on tAsA content of Cr-stressed plants (Fig. 12C), stress led to a significant increase in DHA content by a 2.1-fold increment (Fig. 12D). Depending on these contents, tAsA/DHA decreased under stress exposure, which was a marker for toxicity (Fig. 12E). Cr plus CDs caused an opposite response in the contents of tAsA and DHA. While CD alone (CD1-2-3) resulted in the elevated contents of tAsA, CD addition to plants under the control conditions produced any effect in DHA content. The induced levels of tAsA/DHA were observed under the combined form of Cr and CD1-2-3, which was an indicator of defense response against Cr stress. However, in comparison with those of the Cr stress-treated lettuce plants alone, the increment in tAsA/DHA was not maintained by CD4 (500 mg L^{-1} CD). Cr stress did not change in GSH content (Fig. 12F). On the other hand, the lettuce leaves exposed to Cr stress exhibited a high GSSG content by a 32% increase (Fig. 12G). The high contents of GSH were observed under Cr + CD1-2-3. A remarkable increase in GSSG content was detected only in plants with CD1-2 as compared to the Cr stress alone. As shown in Fig. 12H, the GSH redox state reduced by Cr stress could be preserved by exogenously applied CD1-2-3, but not under Cr + CD4.

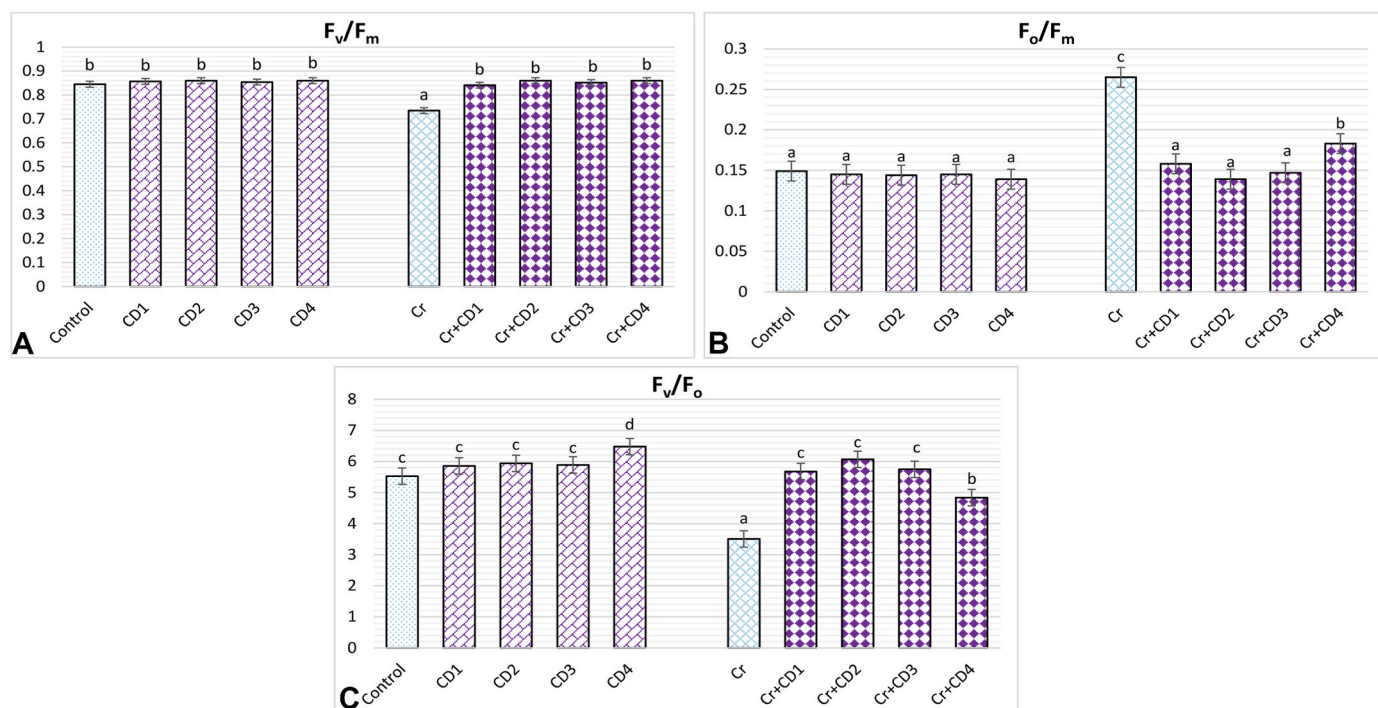


Fig. 5. The effects of orange peel derived-carbon dots (50-100-200-500 mg L⁻¹ CD) on (A) maximal quantum yield of PSII photochemistry (F_v/F_m), (B) physiological state of the photosynthetic apparatus (F_o/F_m), (C) potential photochemical efficiency (F_v/F_o) in lettuce plants under chromium (VI) oxide (100 μM Cr). (For interpretation of the references to colour in this figure legend, the reader is referred to the Web version of this article.)

4. Discussion

CDs were synthesized by a general method accepted in the literature and powdered after the necessary purification steps. Together with the obtained carbon dots, solutions with Cr were given to the plants and their effect was tried to be understood. Carbon dots and plant samples were characterized by fluorescence, FT-IR and XRD spectroscopy. According to the fluorescence spectra, emission peaks were obtained in the samples taken from the plant where the carbon dots alone emit intense peaks, although less intense. In the presence of Cr in the environment, an increase in the emission peaks at the left shoulder peak was observed, and this is thought to be due to the binding between Cr and CD. We can say that Cr (VI) ions are bound due to the presence of amine (NH₂) and carboxyl groups (COO⁻) on the surface of carbon dot (Moonsuang et al., 2020).

According to the analyses, stress reduction in the plant gave better results for the Cr + CD3 composition, where the crystal structure was seen more clearly. The difference in crystal structures emerged as a result of the interactions between the relevant ion-carbon quantum dots as a result of the binding of Cr ions to the surface of the carbon dot and the ion-carbon quantum dot concentration ratios. These results show us that the most appropriate concentration application is 200 mg L⁻¹ for Cr-CD. XRD results show the best reduction in Cr-based stress in sample 3 as seen in all results. The results are consistent with each other.

Elevated accumulation of heavy metals in plants disturbs growth due to altered cell wall components, membrane stability, pigment contents, photosynthesis and ROS overproduction (Chandrakar et al., 2020b). In the present study, the exposure of lettuce plants to Cr toxicity caused a decrement in RGR and RWC due to inhibited cell elongation, and cell division and impairment in the uptake of essential elements such as Singh and Prasad (2019) and Ahmad et al. (2020). CDs as plant growth regulators led to a promotion in the growth and survival of maize plants against drought stress (Yang et al., 2022). Wang et al. (2018) determined that the optimal CD concentration was 200 mg L⁻¹ for growth of mung bean plants, but 1200 mg L⁻¹ CD did not stimulate growth. Similarly, in

our study, all concentrations of CD applied to lettuce plants (50–500 mg L⁻¹) were suitable for good growth levels under the control or Cr stress conditions. CD-triggered growth increments might be connection with induced water dispersion/essential proteins, mineral absorption or nitrogen assimilation/utilization and carbohydrate accumulation/transport by accelerating CO₂ assimilation in photosynthesis (Chen et al., 2020; Kou et al., 2021). Besides, the promoted RGR levels was associated with less accumulation of Cr content under the co-exposure of stress and CD applications. On the other hand, Liang et al. (2023) and Ji et al. (2023) detected that the increased growth in CD-treated plants connected with the root vigor and branch root numbers, which caused the absorption of more water. Wang et al. (2022a) demonstrated the high expression levels of aquaporin genes, PIP1 and PIP2, which play role in water transport under UV-B stress after CD exposure. This result was consistent with the high RWC status under CDs containing hydrophilic groups such as -OH and -COOH, which provide binding sites for water molecules or metal ions (Kou et al., 2021). Being non-enzymatic antioxidant, osmolyte and an amino acid, proline (Pro) regulates the growth by stabilizing the membrane and, controlling protein synthesis and directly quenching free radicals (Saha et al., 2017). In the present study, exogenously applied CDs were effectively reversed through increased Pro content imposed by Cr stress. CD-mediated Pro accumulation under Cr stress could be explained by positive impacts of Pro related to the conservation of redox balance, neutralization ROS and reconstructing chlorophyll, as observed by Emamverdian et al. (2015). This observation in our study was in line with the results of Chandrakar et al. (2020a), which found an induction in Pro content and its biosynthesis gene (pyrroline-5-carboxylate synthetase).

Cr exposure led to a destruction in photosynthesis (Zaheer et al., 2020). Our data showed a critical decline in Mg²⁺ and Mn²⁺ accumulation and unchanged Fe²⁺ contents under Cr stress, which play a role in oxygen-evolving complex and participate in the chlorophyll structure. Similar findings were obtained by Hussain et al. (2018). In the present study, the negative effects induced by stress on stomatal conductance (g_s) and electron transport chain were further intensified due to the

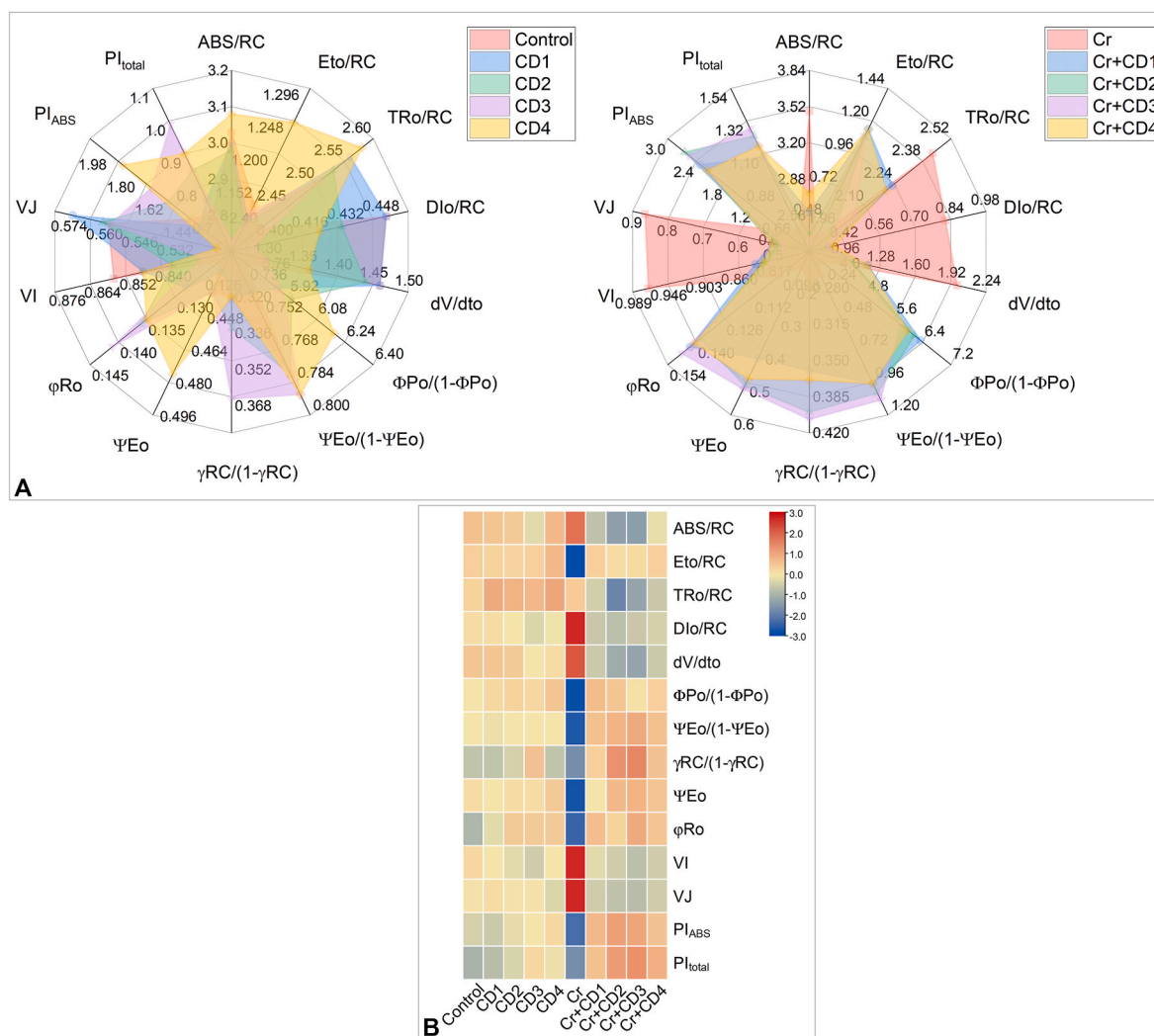


Fig. 6. The effects of orange peel derived-carbon dots (50-100-200-500 mg L⁻¹ CD) chlorophyll *a* transient and heat map in lettuce plants under chromium (VI) oxide (100 μM Cr). **(A)** radar plot with a series parameter derived from JIP-test analyses of the experimental fluorescence OJIP transients: ABS/RC, average absorption per active reaction center; ET_o/RC, electron transport flux per active reaction centers; TR_o/RC, flux or exciton trapped per active reaction center; ΦP_o/(1-ΦP_o), Q_A-reducing RCs per PSII antenna chlorophyll; ΨE_o/(1-ΨE_o), the efficiency with which a trapped exciton transfers an electron to the photosynthetic electron transfer chain; γRC/(1-γRC), Q_A reducing reaction centers per PSII antenna chlorophyll; D_l_o/RC, ratio of total dissipation to the amount of active reaction center; PI_{ABS}, performance index based on the absorption of light energy; PI_{total}, performance index (potential) for energy conservation from exciton to the reduction of PSI and acceptors. **(B)** Heatmap showing correlation among all treatments tested in parameters related to chlorophyll *a* transient. It showed the decreasing change from the red towards the blue. (For interpretation of the references to colour in this figure legend, the reader is referred to the Web version of this article.)

increase in endogenous Cr accumulation. The low levels of g_s showing stomatal closure (Fig. 7A) were better explained by the decreases in A , E and C_i in the stress applied-plants. In parallel with the decrease in Cr stress-induced g_s , the closure of the stomatal opening also limited the assimilation of CO₂ (A , g_s and A/C_i) in photosynthesis and subsequently led to a decline in the yield of lettuce plants. A decrement in photosynthetic products induced by Cr stress might be reflected the reduced RGR levels of lettuce plants. Liang et al. (2023) observed that CD-treated pea seedlings had elevated carbohydrate accumulation, which is a product of photosynthesis as an energy source for growth. In response to UV-B stress, lettuce seedlings had induced net photosynthesis under 0.5 mg mL⁻¹ CD (Wang et al., 2022a). After CD applications to stressed-lettuce plants, stomatal conductance (g_s), transpiration rate (E) and carboxylation efficiency (A/C_i) improved, which correlated with Ji et al. (2023). After CD exposure, the high levels of A/C_i reflected improved CO₂ assimilation rate and removal of Cr-induced stomatal limitation (compatible with the high g_s levels) in lettuce plants. One of the reasons for accelerating CO₂ assimilation was the activation in rubisco enzyme, which improves the carbon reaction process (Guo et al.,

2022a). CDs could maintain the photosynthetic efficiency in the stoma (by reduced L_s) of lettuce plants subjected to Cr toxicity. Therefore, CDs could remove the stomatal and non-stoma restriction in Cr-applied lettuce plants. In more detail to understand the role of CDs on photosynthesis, the interaction of CD applications on the electron transfer among photosystems, chlorophyll fluorescence and dissipation of excess energy accumulated under Cr stress. Concerning chlorophyll fluorescence, F_v/F_m and F_v/F_o were negatively affected by Cr toxicity in lettuce plants, which showed the inactivation in plastoquinone reduction. Our findings were in agreement with the report submitted by Ayyaz et al. (2020). Co-existing of CDs and Cr stress resulted an induction/regulation in quantum yield and electron acceptors of PSII, which caused an eliminating in electron deficiency at PSI, as showed high F_v/F_m and F_v/F_o . Thus, the perturbations in the electron transfer rate in photosystems triggered by Cr stress were removed by CD applications and the redox state of NADP⁺/NADPH in CD-applied lettuce plants could re-controlled by the preventing of over-accumulation of NADPH and H⁺. The reduced F_o/F_m levels observed that CDs caused the low reduction rate of Q_A and modulated the oxidation of Q_B. Depending on F_o/F_m values, CDs could

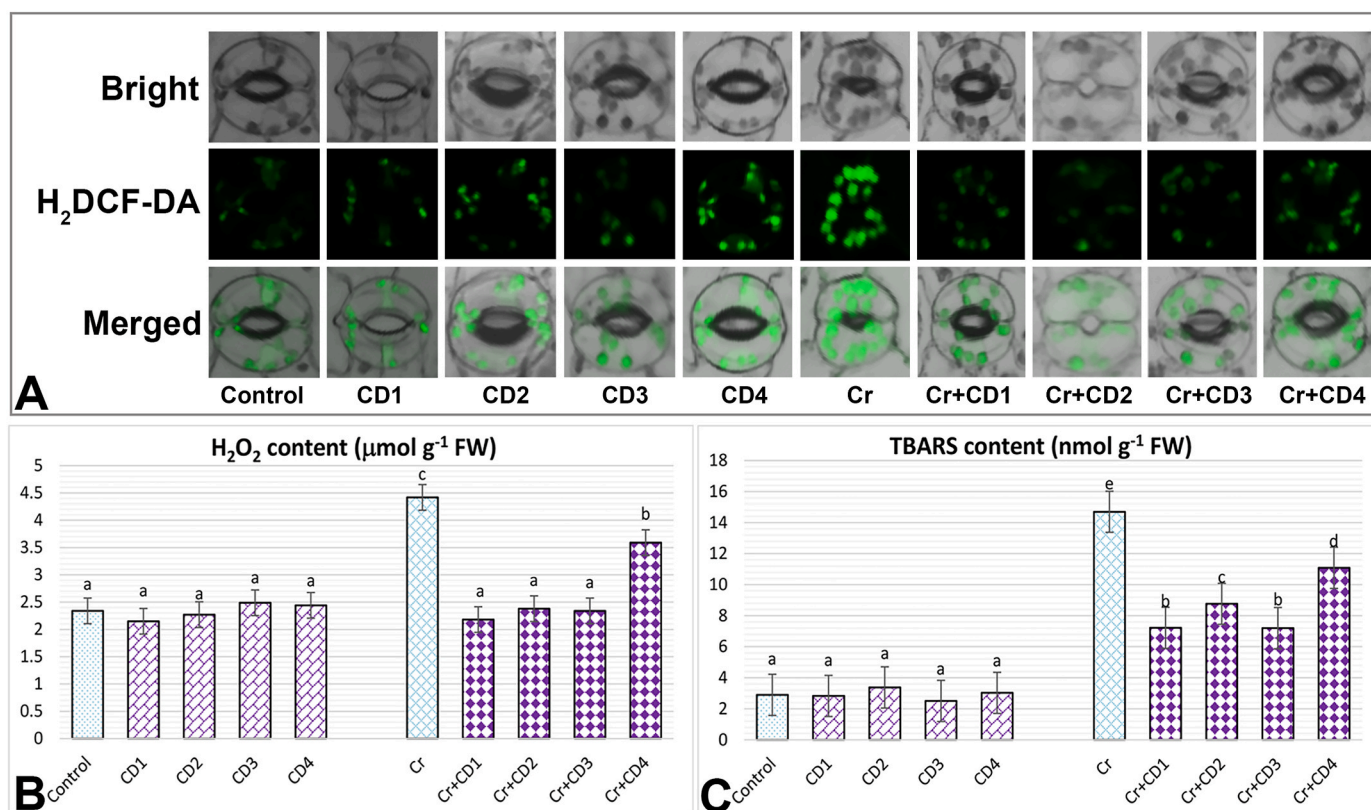


Fig. 7. The effects of orange peel derived-carbon dots (50-100-200-500 mg L⁻¹ CD) on (A) H₂O₂ production (green spots) in stoma after H₂DCF-DA staining, (B) hydrogen peroxide content (H₂O₂), (C) lipid peroxidation (TBARS content) in lettuce plants under chromium (VI) oxide (100 μM Cr). (For interpretation of the references to colour in this figure legend, the reader is referred to the Web version of this article.)

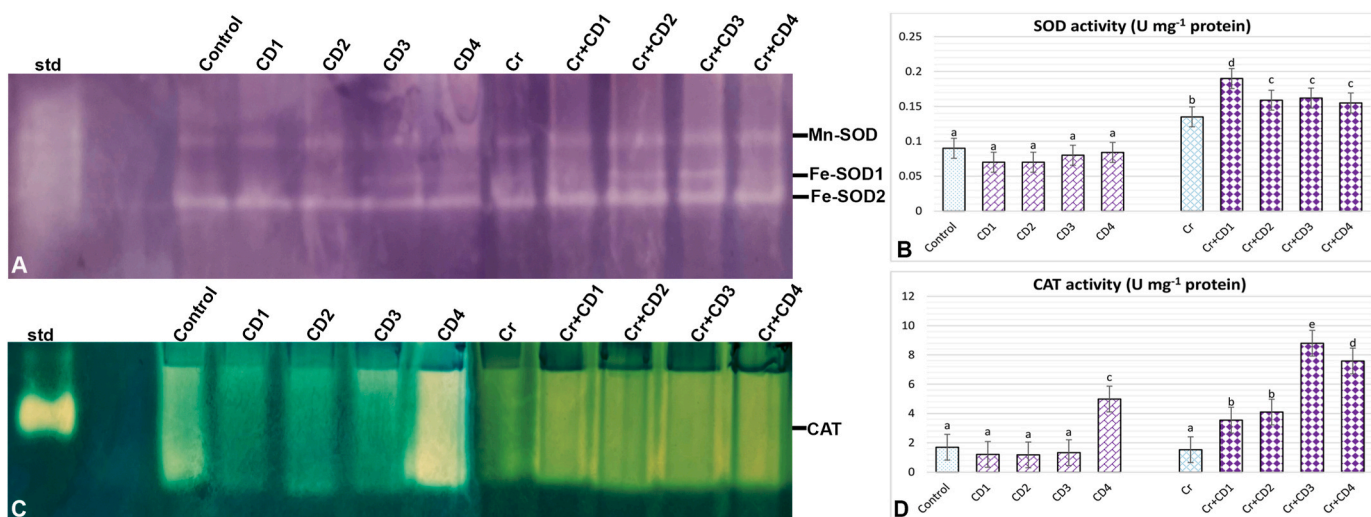


Fig. 8. The effects of orange peel derived-carbon dots (50-100-200-500 mg L⁻¹ CD) on (A) relative band intensity of superoxide dismutase isoenzymes (SOD), (B) total SOD activity, (C) relative band intensity of different types of catalase isoenzymes (CAT), (D) total CAT activity in lettuce plants under chromium (VI) oxide (100 μM Cr). (For interpretation of the references to colour in this figure legend, the reader is referred to the Web version of this article.)

regulate proteins of oxygen evolving complex (OEC) as evident by high endogenous content of Mn²⁺ and F_m under co-exposure of CDs and Cr stress in lettuce plants. Therefore, CDs induced the electron transport rate from OEC to D1 protein, which was related to reaction centers of PSII.

The parameters related to chlorophyll *a* fluorescence transient indicated the absorption flux, electron transport fluxes, trapped/dissipated energy status and performance index of photosynthetic apparatus

under stress or non-stress conditions (Kumar et al., 2020). Our findings showed that Cr toxicity negatively affected energy fluxes (ABS/RC, TR_o/RC, ET_o/RC and DI_o/RC) quantum yields and efficiency (ΨE_o and φR_o) and performance index (PI_{ABS} and PI_{total}) in lettuce plants. Li et al. (2021a) and Wang et al. (2022b) presented encouraging impacts of CDs in growth by increasing PSII efficiency, rubisco activity, chlorophyll content, quantity of light harvesting complex-related gene expression, NADPH production and electron transfer rate (consistent with increased

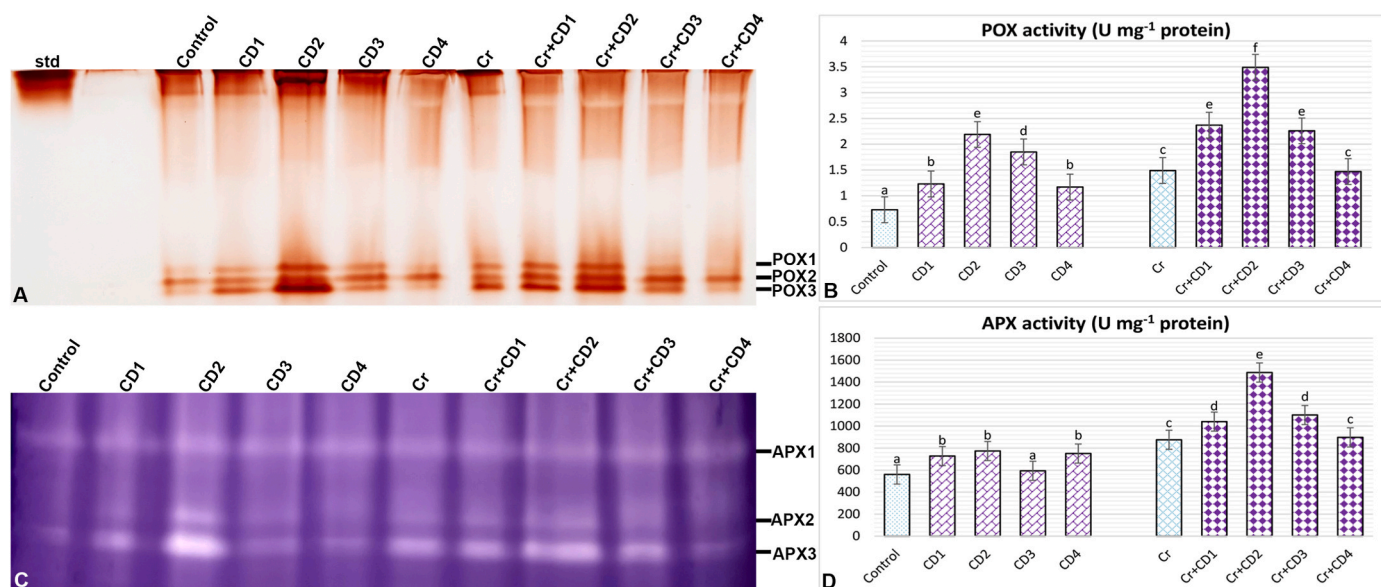


Fig. 9. The effects of orange peel derived-carbon dots (50-100-200-500 mg L⁻¹ CD) on (A) relative band intensity of peroxidase isoforms (POX), (B) total POX activity, (C) relative band intensity of different types of ascorbate peroxidase isoforms (APX), (D) total APX activity in lettuce plants under chromium (VI) oxide (100 μ M Cr). (For interpretation of the references to colour in this figure legend, the reader is referred to the Web version of this article.)

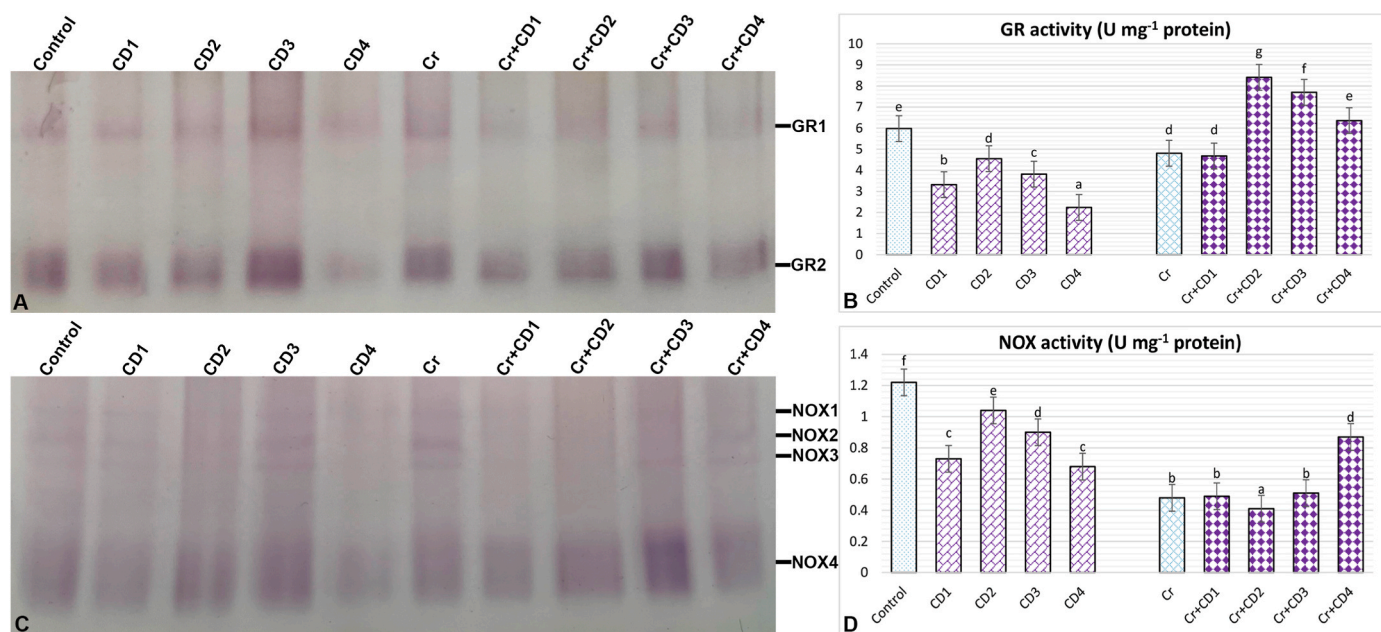


Fig. 10. The effects of orange peel derived-carbon dots (50-100-200-500 mg L⁻¹ CD) on (A) relative band intensity of glutathione reductase isoforms (GR), (B) total GR activity, (C) relative band intensity of different types of NADPH oxidase isoforms (NOX), (D) total NOX activity in lettuce plants under chromium (VI) oxide (100 μ M Cr). (For interpretation of the references to colour in this figure legend, the reader is referred to the Web version of this article.)

ET₀/RC) associated with photosynthetic process in plants. One of the basic reasons for photosynthetic improvements was the induction in light utilization efficiency triggered by CD applications, as suggested by Swift et al. (2019). Like their carboxylation capacity, CDs trigger the efficiency of light energy into NADPH and ATP and optimize the light-capturing antenna system (Xiao et al., 2021). In terms of their photoluminescence properties, Li et al. (2020a) found that CDs can transfer energy to chloroplasts, accelerate the electron transport state in light-harvesting complexes/photosynthetic systems and improve the photosynthetic capacity of chloroplasts in plants exposed to stress. The photosynthetic efficiency and electron transfer rate of PSI (Kou et al., 2021) and PSII (Xiao et al., 2021) are promoted by the addition of CDs.

The declines in ABS/RC in our study interpreted that CDs caused an improvement in the number of active centers of PSII. The absorption flux rate of the reaction center (TR₀/RC and DI₀/RC) induced by Cr stress was re-arranged by all CD applications in lettuce plants. After stress exposure, CDs reduced the dissipation of energy (decreased DI₀/RC) absorbed by PSII and then, energy capture efficiency of PSII increased. In the presence of CD, the removal of induction in d_v/dt₀, V_I and V_J under Cr stress indicated that CDs re-organized the donor side (oxidation) of PSII and improved the antenna efficiency of photosystems in lettuce plants. In the present study, CD-mediated increased values in ϕ Ro and Ψ E₀, which were quantum yield parameters, showed a positive impact on the electron acceptor side in PSI and induced

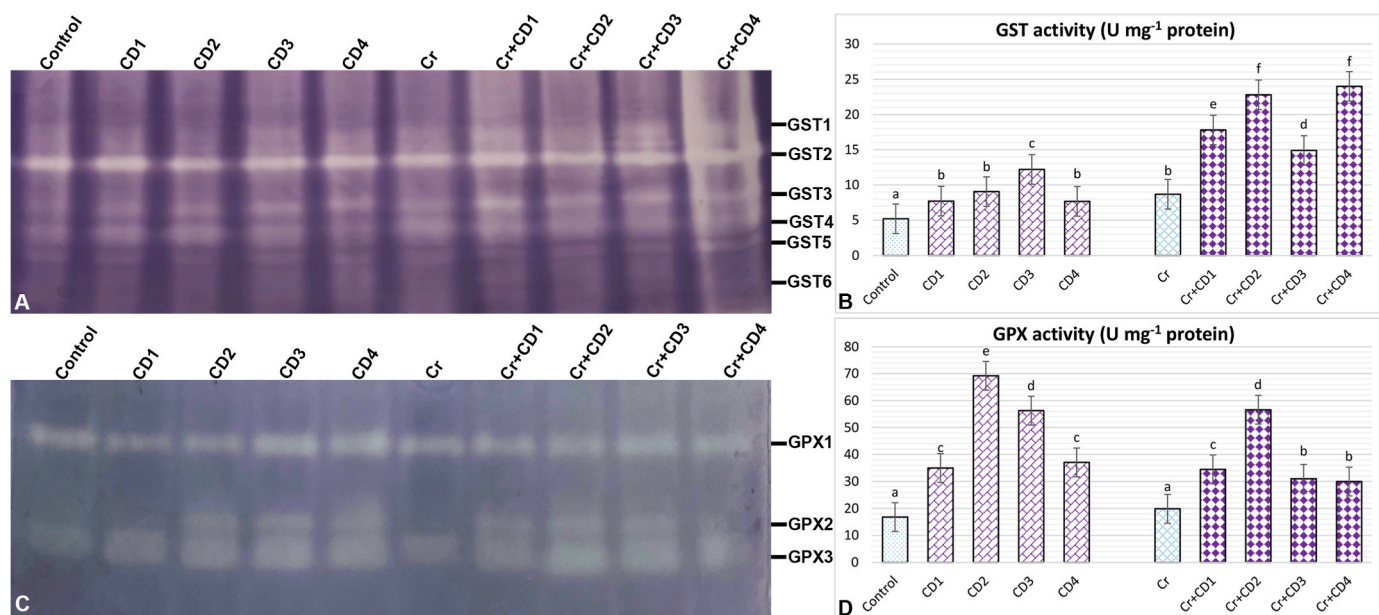


Fig. 11. The effects of orange peel derived-carbon dots (50-100-200-500 mg L⁻¹ CD) on (A) relative band intensity of glutathione S-transferase isoenzymes (GST), (B) total GST activity, (C) relative band intensity of different types of glutathione peroxidase isoenzymes (GPX), (D) total GPX activity in lettuce plants under chromium (VI) oxide (100 μM Cr). (For interpretation of the references to colour in this figure legend, the reader is referred to the Web version of this article.)

ferredoxin-NADP⁺ reductase activity. Besides, the balance of the redox reactions between PSI and PSII was maintained through CD applications as suggested by increasing $\Psi E_o/(1-\Psi E_o)$ against Cr stress. All mentioned impacts of CDs on photosynthetic apparatus resulted in the alleviation of performance indexes (PI_{ABS} and PI_{total}) in photosynthesis under Cr stress by activating PSII repair cycle.

After Cr toxicity, the electrons produced in photolysis are transferred to oxygen, not to NADP⁺, and are formed superoxide anion radicals, which are removed by antioxidant enzymes such as SOD, CAT, POX, APX and GR (Dong et al., 2021). In the present study, the increased SOD activity of Cr-exposed lettuce plants converted from superoxide anion radicals to H₂O₂ and oxygen. For the decomposition of H₂O₂, the only activities of POX and APX were not sufficient. Along with radical accumulation, lipid peroxidation levels (TBARS content) increased in the lettuce plants under Cr toxicity, which caused undesired oxidative damage. The same finding was noted by Farooq et al. (2022), who suggested an arsenic-mediated increase in the TBARS content of *Brassica napus*. Wang et al. (2022a) mentioned that CDs with the oxygen-containing functional groups have increased ROS scavenging ability. The scavenging of radicals by CDs was due to the co-existence of -OH and C=O in CD structure, as suggested by Li et al. (2021a). In the present study, exogenous applied CDs (in all concentrations) activated SOD and CAT enzymes, which was in line with the results of Wang et al. (2022a) under CD plus UV-B stress. Our data showed that POX activity was effective in the elimination of H₂O₂ production under CD treatments, especially at 50-100-200 mg L⁻¹ CD, attributable to reduced H₂O₂ content thus less oxidative damage. NOX localized in the plasma membrane provides the production of superoxide anion radicals by transferring electrons from NADPH to oxygen in the apoplast (Das and Kar, 2018). CDs (except for Cr + CD4) did not supply an increase in NOX activity under the control conditions or Cr stress. A similar diminishment was mentioned by Chandrakar et al. (2020a) under carbon dots plus arsenic stress.

Another defense system is the AsA-GSH cycle, which takes place in the cytoplasm, peroxisomes, chloroplasts and mitochondria in plants (Ma et al., 2015). APX catalyzes H₂O₂ to monodehydroascorbate (MDHA) and water by using AsA as a reducing agent. MDHA and dehydroascorbate (DHA) are catalyzed by MDHAR and DHAR to form AsA, respectively. GSH re-generation is regulated by GR through the

reduction of GSSG (glutathione disulfide), which uses NADPH as an electron donor (Moothoo-Padayachie et al., 2016). As expected, Cr stress caused dramatic declines in the enzyme/non-enzyme activities including the AsA-GSH cycle, except for APX. These changes decreased the redox state of AsA, and GSH, AsA/DHA, GSH/GSSG, which were indicators of Cr stress. To protect the plants against oxidative damage, the redox status of AsA and GSH is maintained under stress conditions. For that reason, after Cr exposure, CDs (50–100 and 200 mg L⁻¹) protected the regeneration of AsA and GSH by increasing activities of APX, GR (except for Cr + CD1), MDHAR and, DHAR, tAsA/DHA and the contents of AsA, and GSH. On the other hand, this trend did not continue under CD4 application (500 mg L⁻¹) in lettuce plants. Interestingly, CD-mediated eliminating capacity of hydroxyl radicals was better than AsA through electron transfer and CDs showed an enzyme-like activity (Wang et al., 2022a). The previous study showed that CD addition to wheat plants under cadmium stress removed the inhibitory effects on GSH synthesis (Xiao et al., 2019). GST and GPX participate actively in the decomposition of H₂O₂ under stress that can conjugate with GSH (Tiwari and Yadav, 2020). In the present study, both activities of GST and GPX contributed to the alleviation of Cr-toxicity by CD applications. Since GSH limited the activity of these enzymes, which caused a decrease in GSH levels at CD4, the contribution of these enzymes for removing H₂O₂ content decreased under CD4 application under Cr stress (Cr + CD4). Nevertheless, in the presence of Cr toxicity, CD applications could lessen the negative impacts of excess H₂O₂ accumulation by activated CAT, POX, GST, GPX and enzymes/non-enzymes related to AsA-GSH cycle depending on CD concentrations. The low levels of H₂O₂ involve in defense responses as a signal molecule by early stomatal closure (Ma et al., 2012). In this study, DCF-DA staining indicated that the low intensity of H₂O₂ fluorescence signed the signal role of H₂O₂ and the scavenging of excess H₂O₂ by the antioxidant system. Besides, CDs decreased the lipid peroxidation in membranes induced by Cr toxicity through activating antioxidant and non-enzymatic systems. So, the decreases in TBARS were observed under Cr plus all CD applications in lettuce plants as indicated by Chandrakar et al. (2020a). Guo et al. (2022b) explained that the reduction of oxidative damage and improvement of antioxidant activity was due to rich in carboxyl groups of CDs.

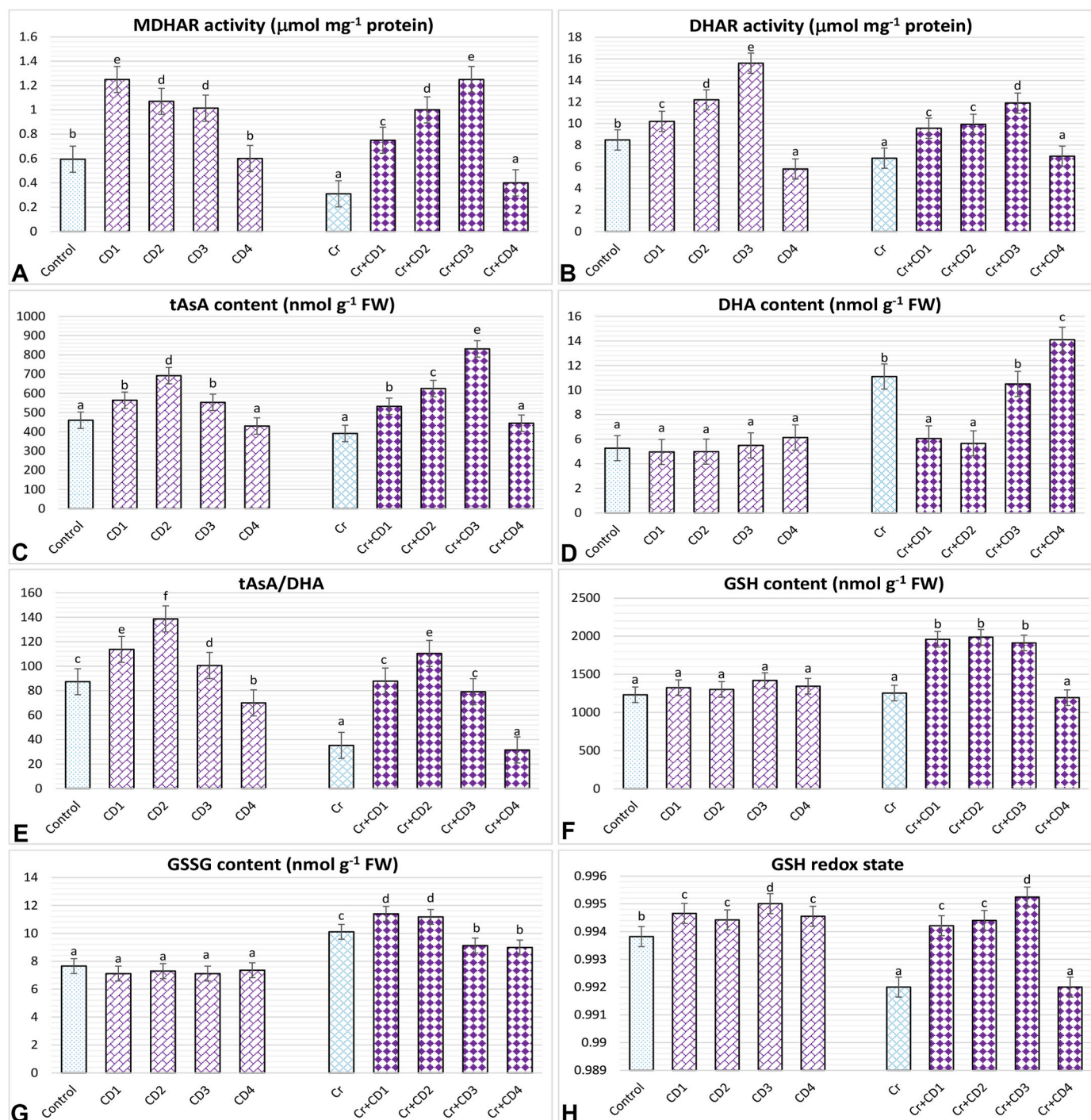


Fig. 12. The effects of different concentrations of orange peel derived-carbon dots ($50\text{-}100\text{-}200\text{-}500\text{ mg L}^{-1}$ CD) on (A) monodehydroascorbate reductase activity (MDHAR), (B) dehydroascorbate reductase activity (DHAR), (C) total ascorbate content (tAsA), (D) dehydroascorbate content (DHA), (E) tAsA/DHA, (F) glutathione content (GSH), (G) oxidized glutathione (GSSG), (H) GSH redox state in lettuce plants under chromium (VI) oxide ($100\text{ }\mu\text{M}$ Cr). (For interpretation of the references to colour in this figure legend, the reader is referred to the Web version of this article.)

5. Conclusion

Our study confirmed that plant-based CDs removed an inhibition on RGR, RWC and Pro content. Cr stress caused declines in photosynthetic efficiency (F_v/F_m , F_v/F_o , and F_o/F_m) in lettuce plants but the improvements in chlorophyll fluorescence were supplied by CD applications. After CD exposure, the high levels of A/C_i reflected improved CO_2 assimilation rate and removal of Cr-induced stomatal limitation (compatible with the changes on g_s , A, E and L_s) in lettuce plants. Cr-

based critical changes in the endogenous contents of Mg^{2+} , Mn^{2+} and Fe^{2+} contents, which play a role in oxygen-evolving complex and participate in the chlorophyll structure and synthesis, were reversed by CD applications. CDs maintained from Cr-induced damages through regulation of the number of active centers of PSII, the absorption flux rate of the reaction center, the balance of the redox reactions between PSI and, PSII and the dissipated energy levels absorbed energy by chlorophyll, as evident by the results of ABS/RC , ET_o/RC , TR_o/RC , DI_o/RC , dV/dt_o , V_i and V_j). All findings associated with photosynthetic

apparatus showed that CDs alleviated the performance indexes (PI_{ABS} and PI_{total}) under Cr stress by activating the PSII repair cycle. By modulating the antioxidant activity (SOD and CAT) in lettuce plants, all CDs were able to remove the toxic levels of H_2O_2 and TBARS produced by stress. Besides, 50-100-200 mg L^{-1} CD activated POX and enzyme/non-enzymes related to the ascorbate-glutathione (AsA-GSH) cycle (APX, monodehydroascorbate reductase (MDHAR) and dehydroascorbate reductase (DHAR), the contents of AsA and, GSH). These CD concentrations were able to protect the AsA regeneration, GSH/GSSG and GSH redox status. Consequently, CDs protected lettuce plants from Cr-induced damages by regulating ion accumulation, gas exchange parameters, antioxidant defense system, electron and energy transfer in photosystems and ROS accumulation.

Funding

Financial support for this work was provided by Selcuk University Scientific Research Projects Coordinating Office and Necmettin Erbakan University Scientific Research Projects Coordinating Office (Project number: 23408008 and 221215001, respectively).

CRediT authorship contribution statement

Ceyda Ozfidan-Konakci: Writing – review & editing, Writing – original draft, Methodology, Investigation. **Evren Yildiztugay:** Writing – review & editing, Writing – original draft, Resources, Methodology, Investigation, Conceptualization. **Busra Arikan-Abdulveli:** Writing – review & editing, Writing – original draft, Methodology, Investigation. **Fatma Nur Alp-Turgut:** Methodology, Investigation. **Canan Baslak:** Investigation, Methodology, Writing – original draft, Writing – review & editing. **Murat Yıldırım:** Writing – review & editing, Writing – original draft, Investigation, Methodology.

Declaration of competing interest

The authors declare that they have no known competing financial interests or personal relationships that could have appeared to influence the work reported in this paper.

Data availability

The authors do not have permission to share data.

Appendix A. Supplementary data

Supplementary data to this article can be found online at <https://doi.org/10.1016/j.chemosphere.2024.141937>.

References

- Ahamed, G.J., Li, X., Yang, Y., Liu, C., Zhou, G., Wan, H., Cheng, Y., 2020. Tomato WRKY81 acts as a negative regulator for drought tolerance by modulating guard cell H_2O_2 -mediated stomatal closure. *Environ. Exp. Bot.* 171, 103960.
- Ahmad, R., Ali, S., Abid, M., Rizwan, M., Ali, B., Tanveer, A., Ahmad, I., Azam, M., Ghani, M.A., 2020. Glycinebetaine alleviates the chromium toxicity in *Brassica oleracea* L. by suppressing oxidative stress and modulating the plant morphology and photosynthetic attributes. *Environ. Sci. Pollut. Control Ser.* 27, 1101–1111.
- Amer, W.A., Rehab, A.F., Abdelghafar, M.E., Torad, N.L., Atlam, A.S., Ayad, M.M., 2021. Green synthesis of carbon quantum dots from purslane leaves for the detection of formaldehyde using quartz crystal microbalance. *Carbon* 179, 159–171.
- Atchudan, R., Edison, T.N.J.L., Shanmugam, M., Perumal, S., Somanathan, T., Lee, Y.R., 2021. Sustainable synthesis of carbon quantum dots from banana peel waste using hydrothermal process for in vivo bioimaging. *Phys. E Low-dimens. Syst. Nanostruct.* 126, 114417.
- Ayyaz, A., Amir, M., Umer, S., Iqbal, M., Bano, H., Gul, H.S., Noor, Y., Javed, M., Athar, H.R., Zafar, Z.U., 2020. Melatonin induced changes in photosynthetic efficiency as probed by OJIP associated with improved chromium stress tolerance in canola (*Brassica napus* L.). *Heliyon* 6, e04364.
- Bajpai, S.K., Souza, A.D., Suhail, B., 2019. Blue light-emitting carbon dots (CDs) from a milk protein and their interaction with *Spinacia oleracea* leaf cells. *Int. Nano Lett.* 9, 203–212.
- Beauchamp, C., Fridovich, I., 1971. Superoxide dismutase: improved assays and an assay applicable to acrylamide gels. *Anal. Biochem.* 44, 276–287.
- Bergmeyer, H.U., 1970. *Methoden der enzymatischen Analyse*. 2. Verlag Chemie.
- Bradford, M.M., 1976. A rapid and sensitive method for the quantitation of microgram quantities of protein utilizing the principle of protein-dye binding. *Anal. Biochem.* 72, 248–254.
- Budak, E., Aykut, S., Paşaoğlu, M.E., Ünlü, C., 2020. Microwave assisted synthesis of boron and nitrogen rich graphitic quantum dots to enhance fluorescence of photosynthetic pigments. *Mater. Today Commun.* 24, 100975.
- Chandrakar, V., Dubey, A., Keshavkant, S., 2016. Modulation of antioxidant enzymes by salicylic acid in arsenic exposed *Glycine max* L. *J. Soil Sci. Plant Nutr.* 16, 662–676.
- Chandrakar, V., Yadu, B., Korram, J., Satnami, M.L., Dubey, A., Kumar, M., Keshavkant, S., 2020a. Carbon dot induces tolerance to arsenic by regulating arsenic uptake, reactive oxygen species detoxification and defense-related gene expression in *Cicer arietinum* L. *Plant Physiol. Biochem.* 156, 78–86.
- Chandrakar, V., Yadu, B., Xalxo, R., Kumar, M., Keshavkant, S., 2020b. Mechanisms of plant adaptation and tolerance to metal/metalloid toxicity. *Plant Ecophysiology and Adaptation under Climate Change: Mechanisms and Perspectives II: Mechanisms of Adaptation and Stress Amelioration* 107–135.
- Chandrasekaran, P., Arul, V., Sethuraman, M.G., 2020. Ecofriendly synthesis of fluorescent nitrogen-doped carbon dots from coccinia grandis and its efficient catalytic application in the reduction of methyl orange. *J. Fluoresc.* 30, 103–112.
- Chen, J., Dou, R., Yang, Z., Wang, X., Mao, C., Gao, X., Wang, L., 2016. The effect and fate of water-soluble carbon nanodots in maize (*Zea mays* L.). *Nanotoxicology* 10, 818–828.
- Chen, J., Liu, B., Yang, Z., Qu, J., Xun, H., Dou, R., Gao, X., Wang, L., 2018. Phenotypic, transcriptional, physiological and metabolic responses to carbon nanodot exposure in *Arabidopsis thaliana* (L.). *Environ. Sci.: Nano* 5, 2672–2685.
- Chen, T., Zhang, H., Zeng, R., Wang, X., Huang, L., Wang, L., Wang, X., Zhang, L., 2020. Shade effects on peanut yield associate with physiological and expressional regulation on photosynthesis and sucrose metabolism. *Int. J. Mol. Sci.* 21, 5284.
- Cheng, L., Li, Y., Zhai, X., Xu, B., Cao, Z., Liu, W., 2014. Polycation-b-polyzwitterion copolymer grafted luminescent carbon dots as a multifunctional platform for serum-resistant gene delivery and bioimaging. *ACS Appl. Mater. Interfaces* 6, 20487–20497.
- Christou, A., Georgiadou, E.C., Zissimos, A.M., Christoforou, I.C., Christofi, C., Neocleous, D., Dalias, P., Torrado, S.O., Argyraki, A., Fotopoulos, V., 2020. Hexavalent chromium leads to differential hormetic or damaging effects in alfalfa (*Medicago sativa* L.) plants in a concentration-dependent manner by regulating nitro-oxidative and proline metabolism. *Environ. Pollut.* 267, 115379.
- Das, S., Kar, R.K., 2018. Abscisic acid mediated differential growth responses of root and shoot of *Vigna radiata* (L.) Wilczek seedlings under water stress. *Plant Physiol. Biochem.* 123, 213–221.
- Dong, W., Chen, D., Chen, Z., Sun, H., Xu, Z., 2021. Antioxidant capacity differences between the major flavonoids in cherry (*Prunus pseudocerasus*) in vitro and in vivo models. *Lwt* 141, 110938.
- Dutilleul, C., Driscoll, S., Cornic, G., De Paepe, R., Foyer, C.H., Noctor, G., 2003. Functional mitochondrial complex I is required by tobacco leaves for optimal photosynthetic performance in photorespiratory conditions and during transients. *Plant Physiol.* 131, 264–275.
- Emamverdian, A., Ding, Y., Mokhberdoran, F., Xie, Y., 2015. Heavy metal stress and some mechanisms of plant defense response. *Sci. World J.* 2015, 756120.
- Fan, Z., Li, S., Yuan, F., Fan, L., 2015. Fluorescent graphene quantum dots for biosensing and bioimaging. *RSC Adv.* 5, 19773–19789.
- Farooq, M.A., Islam, F., Ayyaz, A., Chen, W., Noor, Y., Hu, W., Hannan, F., Zhou, W., 2022. Mitigation effects of exogenous melatonin-selenium nanoparticles on arsenic-induced stress in *Brassica napus*. *Environ. Pollut.* 292, 118473.
- Galal, G.F., Abd-Elhalim, B.T., Abou-Taleb, K.A., Haroun, A.A., Gamal, R.F., 2021. Toxicity assessment of green synthesized Cu nanoparticles by cell-free extract of *Pseudomonas silesiensis* as antitumor cancer and antimicrobial. *Annals of Agricultural Sciences* 66, 8–15.
- Guo, J., Lu, W., Meng, Y., Wang, H., Dong, C., Shuang, S., 2022a. Facile synthesis of multifunctional red-emissive carbon dots for fluorescent quercetin and pH sensing. *Dyes Pigments* 208, 110766.
- Guo, J., Lu, Y., Xie, A.Q., Li, G., Liang, Z.B., Wang, C.F., Yang, X., Chen, S., 2022b. Yellow-emissive carbon dots with high solid-state photoluminescence. *Adv. Funct. Mater.* 32, 2110393.
- Herzog, V., Fahimi, H., 1973. Determination of the activity of peroxidase. *Anal. Biochem.* 55, e62.
- Hildebrandt, N., Spillmann, C.M., Algar, W.R., Pons, T., Stewart, M.H., Oh, E., Susumu, K., Diaz, S.A., Delehanty, J.B., Medintz, I.L., 2017. Energy transfer with semiconductor quantum dot bioconjugates: a versatile platform for biosensing, energy harvesting, and other developing applications. *Chem. Rev.* 117, 536–711.
- Hossain, M., Hossain, M., Fujita, M., 2006. Induction of pumpkin glutathione S-transferases by different stresses and its possible mechanisms. *Biol. Plantarum* 50, 210–218.
- Hu, X., Li, Y., Xu, Y., Gan, Z., Zou, X., Shi, J., Huang, X., Li, Z., Li, Y., 2021. Green one-step synthesis of carbon quantum dots from orange peel for fluorescent detection of *Escherichia coli* in milk. *Food Chem.* 339, 127775.
- Hunt, R., Causton, D.R., Shipley, B., Askew, A.P., 2002. A modern tool for classical plant growth analysis. *Ann. Bot.* 90, 485–488.
- Hussain, A., Ali, S., Rizwan, M., Zia ur Rehman, M., Hameed, A., Hafeez, F., Alamri, S.A., Alyemeni, M.N., Wijaya, L., 2018. Role of zinc-lysine on growth and chromium uptake in rice plants under Cr stress. *J. Plant Growth Regul.* 37, 1413–1422.

- Jaison, A.M.C., Vasudevan, D., Ponmudi, K., George, A., Varghese, A., 2023. One pot hydrothermal synthesis and application of bright-yellow-emissive carbon quantum dots in Hg²⁺ detection. *J. Fluoresc.* 1–14.
- Ji, Y., Yue, L., Cao, X., Chen, F., Li, J., Zhang, J., Wang, C., Wang, Z., Xing, B., 2023. Carbon dots promoted soybean photosynthesis and amino acid biosynthesis under drought stress: reactive oxygen species scavenging and nitrogen metabolism. *Sci. Total Environ.* 856, 159125.
- Jiang, M., Zhang, J., 2002. Involvement of plasma-membrane NADPH oxidase in abscisic acid- and water stress-induced antioxidant defense in leaves of maize seedlings. *Planta* 215, 1022–1030.
- Kou, E., Yao, Y., Yang, X., Song, S., Li, W., Kang, Y., Qu, S., Dong, R., Pan, X., Li, D., 2021. Regulation mechanisms of carbon dots in the development of lettuce and tomato. *ACS Sustain. Chem. Eng.* 9, 944–953.
- Kumar, D., Singh, H., Raj, S., Soni, V., 2020. Chlorophyll a fluorescence kinetics of mung bean (*Vigna radiata* L.) grown under artificial continuous light. *Biochemistry and Biophysics Reports* 24, 100813.
- Kundu, S., Patra, A., 2017. Nanoscale strategies for light harvesting. *Chem. Rev.* 117, 712–757.
- Laemmli, U.K., 1970. Cleavage of structural proteins during the assembly of the head of bacteriophage T4. *Nature* 227, 680–685.
- Le, H.C., Pham, N.T., Vu, D.C., Pham, D.L., Nguyen, S.H., Nguyen, T.T.O., Nguyen, C.D., 2023. Nitrogen-doped graphene quantum dot–tin dioxide nanocomposite ultrathin films as efficient electron transport layers for planar perovskite solar cells. *Crystals* 13, 961.
- LeBlanc, G., Winter, K.M., Crosby, W.B., Jennings, G.K., Cliffel, D.E., 2014. Integration of photosystem I with graphene oxide for photocurrent enhancement. *Adv. Energy Mater.* 4, 1301953.
- Li, H., Huang, J., Lu, F., Liu, Y., Song, Y., Sun, Y., Zhong, J., Huang, H., Wang, Y., Li, S., 2018. Impacts of carbon dots on rice plants: boosting the growth and improving the disease resistance. *ACS Appl. Bio Mater.* 1, 663–672.
- Li, J., Xiao, L., Cheng, Y., Cheng, Y., Wang, Y., Wang, X., Ding, L., 2019. Applications of carbon quantum dots to alleviate Cd²⁺ phytotoxicity in *Citrus maxima* seedlings. *Chemosphere* 236, 124385.
- Li, Q., Wei, Z., Gao, D., Si, P., Yu, H., Liu, J., 2021a. Effects of herbicide drift on chlorophyll fluorescence and antioxidant enzyme levels of various types of fruit trees. *Pakistan J. Bot.* 53, 847–857.
- Li, Y., Xu, X., Wu, Y., Zhuang, J., Zhang, X., Zhang, H., Lei, B., Hu, C., Liu, Y., 2020a. A review on the effects of carbon dots in plant systems. *Mater. Chem. Front.* 4, 437–448.
- Li, Z., Li, Q., Li, R., Zhao, Y., Geng, J., Wang, G., 2020b. Physiological responses of lettuce (*Lactuca sativa* L.) to microplastic pollution. *Environ. Sci. Pollut. Control Ser.* 27, 30306–30314.
- Li, Z., Wang, Q., Zhou, Z., Zhao, S., Zhong, S., Xu, L., Gao, Y., Cui, X., 2021b. Green synthesis of carbon quantum dots from corn stalk shell by hydrothermal approach in near-critical water and applications in detecting and bioimaging. *Microchem. J.* 166, 106250.
- Liang, L., Wong, S.C., Lisak, G., 2023. Effects of plastic-derived carbon dots on germination and growth of pea (*Pisum sativum*) via seed nano-priming. *Chemosphere* 316, 137868.
- Liang, Q., Wang, Y., Lin, F., Jiang, M., Li, P., Huang, B., 2017. A facile microwave-hydrothermal synthesis of fluorescent carbon quantum dots from bamboo tar and their application. *Anal. Methods* 9, 3675–3681.
- Liu, C., Zhang, P., Zhai, X., Tian, F., Li, W., Yang, J., Liu, Y., Wang, H., Wang, W., Liu, W., 2012. Nano-carrier for gene delivery and bioimaging based on carbon dots with PEI-passivation enhanced fluorescence. *Biomaterials* 33, 3604–3613.
- Liu, M.L., Yang, L., Li, R.S., Chen, B.B., Liu, H., Huang, C.Z., 2017. Large-scale simultaneous synthesis of highly photoluminescent green amorphous carbon nanodots and yellow crystalline graphene quantum dots at room temperature. *Green Chem.* 19, 3611–3617.
- Ma, J., Lv, C., Xu, M., Chen, G., Lv, C., Gao, Z., 2016. Photosynthesis performance, antioxidant enzymes, and ultrastructural analyses of rice seedlings under chromium stress. *Environ. Sci. Pollut. Control Ser.* 23, 1768–1778.
- Ma, J., Zheng, G., Pei, C., Zhang, Z., 2015. The function of ascorbate-glutathione cycle in salt tolerance of alfalfa mutant. *Plant Physiol.* 51, 1749–1756.
- Lu, K.Q., Quan, Q., Zhang, N., Xu, Y.Z., 2016. Multifarious roles of carbon quantum dots in heterogeneous photocatalysis. *J. Energy Chem.* 25 (6), 927–935.
- Ma, Y., An, Y., Shui, J., Sun, Z., 2011. Adaptability evaluation of switchgrass (*Panicum virgatum* L.) cultivars on the Loess Plateau of China. *Plant Sci.* 181, 638–643.
- Ma, Y., She, X., Yang, S., 2012. Sphingosine-1-phosphate (S1P) mediates darkness-induced stomatal closure through raising cytosol pH and hydrogen peroxide (H₂O₂) levels in guard cells in *Vicia faba*. *Sci. China Life Sci.* 55, 974–983.
- Maghsoodi, K., Arvin, M.J., Ashraf, M., 2019. Mitigation of arsenic toxicity in wheat by the exogenously applied salicylic acid, 24-epi-brassinolide and silicon. *J. Soil Sci. Plant Nutr.* 20, 577–588.
- Mittler, R., Zilinskas, B.A., 1993. Detection of ascorbate peroxidase-activity in native gels by inhibition of the ascorbate-dependent reduction of nitroblue tetrazolium. *Anal. Biochem.* 212, 540–546.
- Moonsuang, B., Thaitong, B., Amonpattaratkit, P., Praingam, N., Prayongpan, P., 2020. X-ray absorption spectroscopy examination of Cr, Co, and Cu binding on fluorescent carbon dots. *Radiat. Phys. Chem.* 172, 108751.
- Moothoo-Padayachie, A., Varghese, B., Pammenter, N.W., Govender, P., Sershen, 2016. Germination associated ROS production and glutathione redox capacity in two recalcitrant-seeded species differing in seed longevity. *Botany* 94, 1103–1114.
- Muktha, H., Sharath, R., Kottam, N., Smrithi, S., Samrat, K., Ankitha, P., 2020. Green synthesis of carbon dots and evaluation of its pharmacological activities. *BioNanoScience* 10, 731–744.
- Nabiev, I., Rakovich, A., Sukhanova, A., Lukashev, E., Zagidullin, V., Pachenko, V., Rakovich, Y.P., Donegan, J.F., Rubin, A.B., Govorov, A.O., 2010. Fluorescent quantum dots as artificial antennas for enhanced light harvesting and energy transfer to photosynthetic reaction centers. *Angew. Chem. Int. Ed.* 49, 7217–7221.
- Nakano, Y., Asada, K., 1981. Hydrogen peroxide is scavenged by ascorbate-specific peroxidase in spinach chloroplasts. *Plant Cell Physiol.* 22, 867–880.
- Nyomora, A., Sah, R., Brown, P.H., Miller, R., 1997. Boron determination in biological materials by inductively coupled plasma atomic emission and mass spectrometry: effects of sample dissolution methods. *Fresen. J. Anal. Chem.* 357, 1185–1191.
- Oliveira, E.G.d.L., de Oliveira, H.P., Gomes, A.S., 2020. Metal nanoparticles/carbon dots nanocomposites for SERS devices: Trends and perspectives. *SN Appl. Sci.* 2, 1–11.
- Panahirad, S., Dadpour, M., Gohari, G., Akbari, A., Mahdavinia, G., Jafari, H., Kulak, M., Alcázar, R., Fotopoulos, V., 2023. Putrescine-functionalized carbon quantum dot (put-CQD) nanoparticle: a promising stress-protecting agent against cadmium stress in grapevine (*Vitis vinifera* cv. *sultana*). *Plant Physiol. Biochem.* 197, 107653.
- Paradiso, A., Berardino, R., de Pinto, M.C., Sanita di Toppi, L., Storelli, M.M., Tommasi, F., De Gara, L., 2008. Increase in ascorbate-glutathione metabolism as local and precocious systemic responses induced by cadmium in durum wheat plants. *Plant Cell Physiol.* 49, 362–374.
- Prakash, V., Rai, P., Sharma, N.C., Singh, V.P., Tripathi, D.K., Sharma, S., Sahi, S., 2022. Application of zinc oxide nanoparticles as fertilizer boosts growth in rice plant and alleviates chromium stress by regulating genes involved in oxidative stress. *Chemosphere* 303, 134554.
- Prasanna, A., Imae, T., 2013. One-pot synthesis of fluorescent carbon dots from orange waste peels. *Ind. Eng. Chem. Res.* 52, 15673–15678.
- Qu, S., Wang, X., Lu, Q., Liu, X., Wang, L., 2012. A biocompatible fluorescent ink based on water-soluble luminescent carbon nanodots. *Angew. Chem. Int. Ed.* 51, 12215–12218.
- Rao, K.M., Sresty, T., 2000. Antioxidative parameters in the seedlings of pigeonpea (*Cajanus cajan* (L.) Millspaugh) in response to Zn and Ni stresses. *Plant Sci.* 157, 113–128.
- Ricci, G., Bello, M.L., Caccuri, A.M., Galiazzi, F., Federici, G., 1984. Detection of glutathione transferase activity on polyacrylamide gels. *Anal. Biochem.* 143, 226–230.
- Sabet, M., Mahdavi, K., 2019. Green synthesis of high photoluminescence nitrogen-doped carbon quantum dots from grass via a simple hydrothermal method for removing organic and inorganic water pollution. *Appl. Surf. Sci.* 463, 283–291.
- Sagi, M., Fluhr, R., 2001. Superoxide production by plant homologues of the gp91phox NADPH oxidase. Modulation of activity by calcium and by tobacco mosaic virus infection. *Plant Physiol.* 126, 1281–1290.
- Saha, J., Majumder, B., Muntaz, B., Biswas, A.K., 2017. Arsenic-induced oxidative stress and thiol metabolism in two cultivars of rice and its possible reversal by phosphate. *Acta Physiol. Plant.* 39, 1–20.
- SeEVERS, P., DALY, J., CATEDRAL, F., 1971. The role of peroxidase isozymes in resistance to wheat stem rust disease. *Plant Physiol.* 48, 353–360.
- Shahriari, M., Zibae, A., Shamakhi, L., Sahebzadeh, N., Naseri, D., Hoda, H., 2019. Bio-efficacy and physiological effects of *Eucalyptus globulus* and *Allium sativum* essential oils against *Ephesia kuehniella* Zeller (Lepidoptera: Pyralidae). *Toxin Rev.* 39 (4), 422–433.
- Shi, H., Ye, T., Chan, Z., 2013. Exogenous application of hydrogen sulfide donor sodium hydrosulfide enhanced multiple abiotic stress tolerance in bermudagrass (*Cynodon dactylon* (L.) Pers.). *Plant Physiol. Biochem.* 71, 226–234.
- Siddique, A.B., Pramanick, A.K., Chatterjee, S., Ray, M., 2018. Amorphous carbon dots and their remarkable ability to detect 2, 4, 6-trinitrophenol. *Sci. Rep.* 8, 9770.
- Singh, S., Prasad, S.M., 2019. Regulation of chromium toxicity tolerance in tomato and brinjal by calcium and sulfur through nitric oxide: Involvement of enzymes of sulfur assimilation and the ascorbate-glutathione cycle. *Environ. Exp. Bot.* 166, 103789.
- Su, L.X., Ma, X.L., Zhao, K.K., Shen, C.L., Lou, Q., Yin, D.M., Shan, C.X., 2018. Carbon nanodots for enhancing the stress resistance of peanut plants. *ACS Omega* 3, 17770–17777.
- Su, Y., Zhang, M., Zhou, N., Shao, M., Chi, C., Yuan, P., Zhao, C., 2017. Preparation of fluorescent N, P-doped carbon dots derived from adenosine 5'-monophosphate for use in multicolor bioimaging of adenocarcinomic human alveolar basal epithelial cells. *Microchim. Acta* 184, 699–706.
- Swift, T.A., Oliver, T.A., Galan, M.C., Whitney, H.M., 2019. Functional nanomaterials to augment photosynthesis: evidence and considerations for their responsible use in agricultural applications. *Journal of the Royal Society Interface Focus* 9, 20180048.
- Tan, T.L., Zulkifli, N.A., Zaman, A.S.K., binti Jusoh, M., Yaapar, M.N., Rashid, S.A., 2021. Impact of photoluminescent carbon quantum dots on photosynthesis efficiency of rice and corn crops. *Plant Physiol. Biochem.* 162, 737–751.
- Tiwari, Y.K., Yadav, S.K., 2020. Effect of high-temperature stress on ascorbate-glutathione cycle in maize. *Agric. Res.* 9, 179–187.
- Velikova, V., Yordanov, I., Edreva, A., 2000. Oxidative stress and some antioxidant systems in acid rain-treated bean plants: protective role of exogenous polyamines. *Plant Sci.* 151, 59–66.
- Wang, B., Song, H., Qu, X., Chang, J., Yang, B., Lu, S., 2021. Carbon dots as a new class of nanomedicines: opportunities and challenges. *Coord. Chem. Rev.* 442, 214010.
- Wang, H., Kang, Y., Yang, N., Li, H., Huang, S., Liang, Z., Zeng, G., Huang, Y., Li, W., Zheng, M., 2022a. Inhibition of UV-B stress in lettuce through enzyme-like *Scutellaria baicalensis* carbon dots. *Ecotoxicol. Environ. Saf.* 246, 114177.
- Wang, H., Zhang, M., Song, Y., Li, H., Huang, H., Shao, M., Liu, Y., Kang, Z., 2018. Carbon dots promote the growth and photosynthesis of mung bean sprouts. *Carbon* 136, 94–102.
- Wang, J.W., Liu, Y., Xu, Y.X., Chen, W.J., Han, Y.N., Wang, G.G., Jin, S.H., 2022b. Sexual differences in gas exchange and chlorophyll fluorescence of *Torreya grandis* under drought stress. *Trees Struct. Funct.* 36, 283–294.

- Woodbury, W., Spencer, A., Stahmann, M., 1971. An improved procedure using ferricyanide for detecting catalase isozymes. *Anal. Biochem.* 44, 301–305.
- Xiao, L., Guo, H., Wang, S., Li, J., Wang, Y., Xing, B., 2019. Carbon dots alleviate the toxicity of cadmium ions (Cd^{2+}) toward wheat seedlings. *Environ. Sci.: Nano* 6, 1493–1506.
- Xiao, L., Liu, G., Gong, F., Zhu, H., Zhang, Y., Cai, Z., Li, Y., 2021. A minimized synthetic carbon fixation cycle. *ACS Catal.* 12, 799–808.
- Yang, H., Wang, C., Chen, F., Yue, L., Cao, X., Li, J., Zhao, X., Wu, F., Wang, Z., Xing, B., 2022. Foliar carbon dot amendment modulates carbohydrate metabolism, rhizospheric properties and drought tolerance in maize seedling. *Sci. Total Environ.* 809, 151105.
- Zaheer, I.E., Ali, S., Saleem, M.H., Imran, M., Alnusairi, G.S., Alharbi, B.M., Riaz, M., Abbas, Z., Rizwan, M., Soliman, M.H., 2020. Role of iron-lysine on morpho-physiological traits and combating chromium toxicity in rapeseed (*Brassica napus* L.) plants irrigated with different levels of tannery wastewater. *Plant Physiol. Biochem.* 155, 70–84.
- Zhang, H.Y., Wang, Y., Xiao, S., Wang, H., Wang, J.H., Feng, L., 2017. Rapid detection of Cr (VI) ions based on cobalt (II)-doped carbon dots. *Biosens. Bioelectron.* 87, 46–52.
- Zhang, M., Hu, L., Wang, H., Song, Y., Liu, Y., Li, H., Shao, M., Huang, H., Kang, Z., 2018. One-step hydrothermal synthesis of chiral carbon dots and their effects on mung bean plant growth. *Nanoscale* 10, 12734–12742.
- Zhao, S., Lan, M., Zhu, X., Xue, H., Ng, T.W., Meng, X., Lee, C.S., Wang, P., Zhang, W., 2015. Green synthesis of bifunctional fluorescent carbon dots from garlic for cellular imaging and free radical scavenging. *ACS Appl. Mater. Interfaces* 7, 17054–17060.
- Zhao, Y., Hu, C., Wang, X., Qing, X., Wang, P., Zhang, Y., Zhang, X., Zhao, X., 2019. Selenium alleviated chromium stress in Chinese cabbage (*Brassica campestris* L. ssp. *pekinensis*) by regulating root morphology and metal element uptake. *Ecotoxicol. Environ. Saf.* 173, 314–321.